

INTERMODULATION DISTORTION IN A BROAD BAND BALANCED MIXER

by

ROBERT EARL SNYDER

B.S., Cornell University  
(1967)

SUBMITTED IN PARTIAL FULFILLMENT OF THE  
REQUIREMENTS FOR THE DEGREE OF  
MASTER OF SCIENCE  
at the  
MASSACHUSETTS INSTITUTE OF TECHNOLOGY  
March, 1969

Signature of Author                       
Department of Electrical Engineering, March 27, 1969

Certified by                     

Accepted by                       
Chairman, Departmental Committee on Graduate Students



# INTERMODULATION DISTORTION IN A BROAD BAND BALANCED MIXER

by

ROBERT EARL SNYDER

Submitted to the Department of Electrical  
Engineering on March 28, 1969, in partial  
fulfillment of the requirements for the  
Degree of Master of Science

## ABSTRACT

A theory for third-order intermodulation (IM) distortion in broad band doubly balanced mixers using Schottky barrier diodes is derived. This theory is based on the assumption that only two sources of distortion are present: IM due to forward biased diode non-linear conduction, and that due to reverse biased diode non-linear capacitance.

Measurements are made in the high frequency spectrum, both on IM generated in single diodes and that generated in the mixers themselves. Close agreement with theory is found for the single diodes in forward and reverse bias, within given limits on the bias level. The mixer IM is approximately 10 db larger than the theory predicts; this discrepancy is attributed to the presence of IM distortion generated in the diode transition region.

It is found that use of a square wave local oscillator results in up to 20 db reduction of IM distortion over a sine wave LO in the mixers. The existence of an optimum mixer source impedance for minimum IM distortion is shown, thus confirming the theoretical prediction.

THESIS SUPERVISOR: Donald H. Steinbrecher  
TITLE: Research Associate

## ACKNOWLEDGMENT

The author wishes to express his deepest thanks to Dr. Donald H. Steinbrecher, without whose help and guidance this thesis would not have been possible.

Thanks are also due Professor Robert P. Rafuse for his stimulating discussions and comments.

Final thanks to the staff of the Research Laboratory of Electronics, the members of the Solid State Microwave Electronics Group, and Adams-Russell, Inc. for their generous assistance in all phases of this thesis.

## TABLE OF CONTENTS

	Page
Introduction	5
Theory	8
Sources of IM Distortion in Balanced Mixers	8
IM In Forward Conduction	11
IM In Reverse Capacitance	12
IM In Reverse Conduction	15
IM In The Transition Region	15
Other Sources of IM	17
The Two-State Assumption on Mixer IM	18
Mixer IM In Forward Biased Diodes	20
Mixer IM In Reversed Biased Diodes	23
Two-State Mixer IM	25
Experiment	29
Diode Parameter Measurements	29
Test Mixer Construction and Performance	37
Measurement of IM Distortion	47
IM Ratio in Diodes	52
IM Ratio in Mixers	71
Conclusions	79
Footnotes	82
Other References	83

## INTERMODULATION DISTORTION IN A BROAD BAND BALANCED MIXER

### INTRODUCTION

The first mixer in a wide band receiver is frequently subjected to a very wide range of signals from the antenna or any stages of RF amplification. These signals might range from less than one microvolt to more than one volt in amplitude. A prime test of this mixer's quality is its ability to process the widest possible signal amplitude range without distortion; that is, that it have the widest possible dynamic range. A mixer's ability to process weak signals is determined by its noise figure, the receiver noise bandwidth, and the required signal-to-noise ratio. Strong signals can interact with each other due to nonlinearities in the mixer and produce distortion products which can interfere with weak signal detection. A useful definition of dynamic range for a mixer, or other devices, is thus the ratio of the minimum signal power necessary to achieve a given signal-to-noise ratio, to the maximum signal power before distortion products achieve that signal-to-noise ratio.

An important form of distortion in mixers and other devices is intermodulation, or IM, distortion, which occurs when large signals at two different frequencies interact to produce distortion at still other frequencies. As will be seen, third order IM distortion occurs when two signals at frequencies  $f_1$  and  $f_2$  interact to produce distortion power at frequencies  $2f_2 \pm f_1$  and  $2f_1 \pm f_2$ . Note that if  $f_1$  and  $f_2$  are arbitrarily close to one another, then two of the

third order IM signals are arbitrarily close to the input signal frequencies. Thus, even with filtering at the receiver input, third order IM distortion can still be a problem.

It is apparent, then, that a good understanding of the mechanism of distortion production, especially that of IM distortion, in mixers is important to wide dynamic range receiver design. It would be desirable to have a theory for IM production which is simple enough to use as a design tool for minimizing IM distortion, yet accurate. In this thesis a simple theory is derived for third order IM distortion in a broad band doubly balanced, so-called ring, mixer using Schottky barrier diodes. This mixer is chosen for study because it is simple, possessing no tuned circuitry, and very widely used. The doubly balanced mixer has the advantage that, due to its symmetry, the RF, IF, and LO ports are all isolated from each other. The theory is based on the mixer diode nonlinearities, and is written in terms of the diode parameters. The individual sources of IM distortion in the diodes are discussed. Then the assumption is made that only two of these sources are significant; these are combined to produce a formula for the percentage of third order IM distortion power at the mixer output.

An experimental evaluation of the theory follows the derivation. The diode parameters are first determined from low frequency measurements. Then the IM distortion is investigated in single diodes, source by source.

Finally the diodes are placed in mixers and the mixer IM distortion is measured. This experimental investigation is carried on in 2 to 100 MHz frequency band, principally because of ease of component construction in this range.

## THEORY

### SOURCES OF IM DISTORTION IN BALANCED MIXERS

The schematic of a conventional doubly balanced mixer is shown in Fig. 1. The operation of this mixer has been discussed elsewhere in detail;<sup>1,2,3</sup> therefore, a brief discussion will suffice here. The local oscillator signal is fed into the port labeled LO. Since this port is connected to the center taps of the input and output hybrid transformers, it is apparent that the local oscillator "sees" the four diodes as in Fig. 1a, that is, parallel diode pairs back-to-back. Thus, if the local oscillator power is sufficiently high, during the positive half cycle of the local oscillator, diodes 1 and 2 are biased on, while diodes 3 and 4 are biased off; this condition is reversed in the negative half cycle. We can think of the four diodes in an ideal mixer, then, as a reversing switch operated at the LO rate. A signal of frequency of RF entering the RF port is observed at the IF port to be reversed in sign at the LO rate, that is, the RF signal is multiplied by a square wave function of period  $1/f_{LO}$ , where  $f_{LO}$  is the local oscillator frequency, and amplitude equal to 1. Thus, frequency translation of the input signal takes place; signals at frequencies  $f_{RF} \pm n f_{LO}$ , where  $n$  is an odd integer, appear at the IF port, because the square wave is composed of odd numbered harmonics of the LO frequency. If the hybrids and terminations in the mixer are infinitely fast switches, then the mixer will be infinitely broad band.



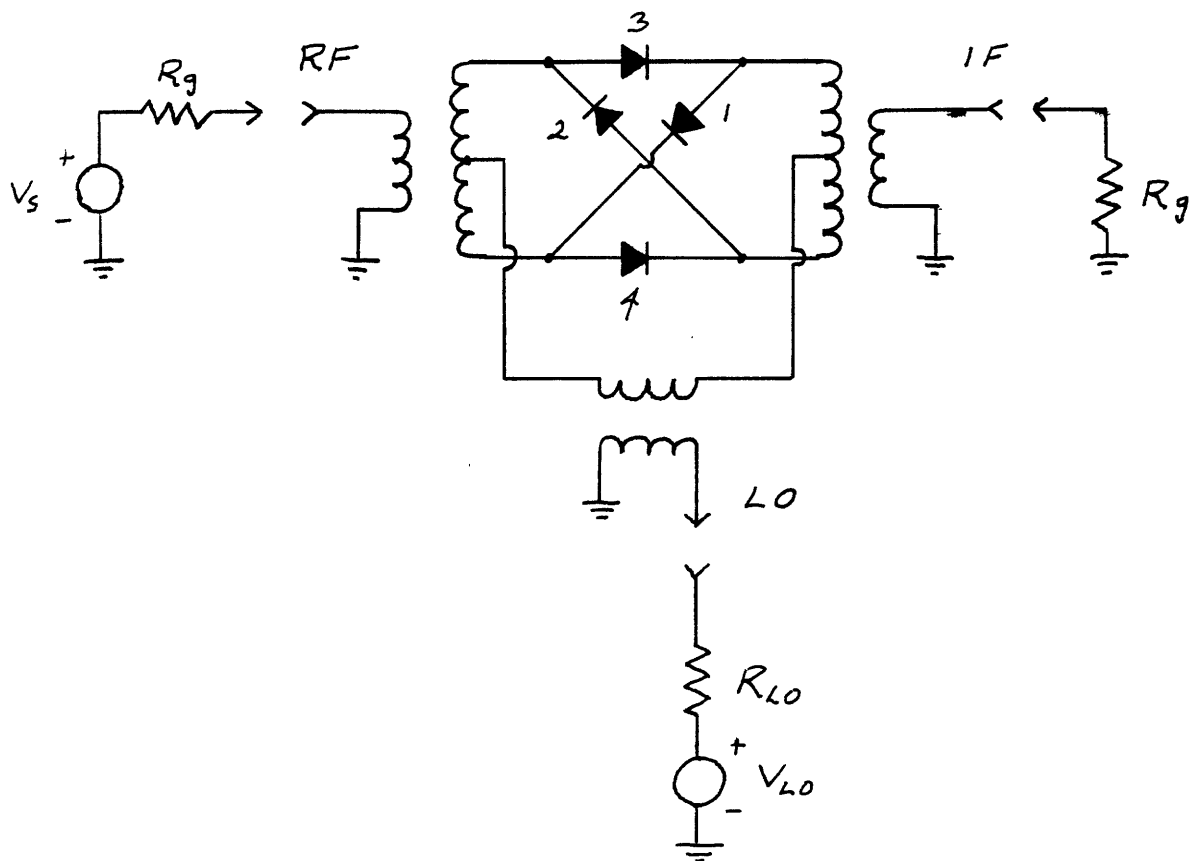


FIG. 1 DOUBLY BALANCED MIXER SCHEMATIC

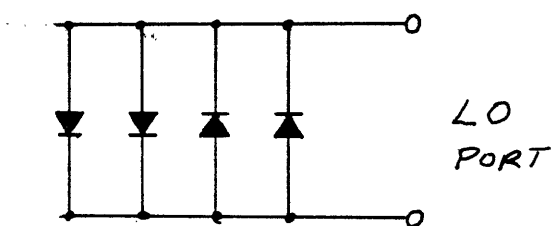


FIG. 1a DIODES AS SEEN FROM LO PORT

Unfortunately, however, real-world diodes are not ideal switches. In both the "on" and "off" states, the voltage across a diode is a non-linear function of the current through the diode. In general, this dependence can be written in a power series; thus:

$$v = a_1 i + a_2 i^2 + a_3 i^3 + \dots \quad (1)$$

where  $i$  and  $v$  are the diode current and voltage, respectively, and the  $a_k$ 's are constants dependent upon the operating region at which the diode is biased. As will be seen in subsequent analyses, if a current of the form

$$i = I_1 \cos \omega_1 t + I_2 \cos \omega_2 t$$

flows through the diode, then the cubic term in Eq. 1 dictates that the diode voltage has components at frequencies  $2\omega_1 \pm \omega_2$  and  $2\omega_2 \pm \omega_1$ . These voltages are known as the third order intermodulation (IM) distortion voltages. Thus a distortion voltage will appear across the load termination at the IF port of a mixer. A convenient measure of the distortion level is the third order intermodulation distortion ratio (IMR), defined as the ratio of power dissipated in the IF termination at one of the third order IM frequencies, to the power dissipated at one of the input frequencies,  $\omega_1$  or  $\omega_2$ .

Several sources of IM distortion exist in a mixer, each corresponding to a region of operation of the mixer diodes. Schottky barrier diodes are used in the analyses and in the mixers, principally because these diodes are majority carrier devices, unlike P-N junction diodes, so they have extremely rapid switching speeds and are thus a

closer approximation to the ideal switch than are P-N diodes. The physical operation of Schottky barrier diodes is described elsewhere.<sup>4,5</sup> The results of these descriptions will be used to describe the various sources of IM distortion below.

## IM IN FORWARD CONDUCTION

The physical model for a Schottky barrier diode in forward conduction is the diode junction in series with a resistance  $R_s$  whose value is independent of forward current. The voltage  $V$  across the junction is related to the forward current  $I$  by

$$V = \frac{1}{\alpha} (\ln I - \ln I_{SAT}) \quad (2)$$

where  $\alpha$  and  $I_{SAT}$  are parameters independent of forward current. If we assume that the diode is biased by the local oscillator to some operating point  $(I_o, V_o)$  in the forward conducting region, as shown in Fig. 2, and that some small RF current is made to flow through the diode, then we may model this condition by expanding Eq. 2 in a Taylor series:

$$V = V_o + \nu_1 (I - I_o) + \frac{\nu_2}{2!} (I - I_o)^2 + \frac{\nu_3}{3!} (I - I_o)^3 + \dots \quad (3)$$

where  $\nu_k = \frac{d^k V}{dI^k}$  evaluated at  $I = I_o$ .

That is,  $\nu_1 = \frac{1}{\alpha I_o}$ ,  $\nu_2 = -\frac{1}{\alpha I_o^2}$ ,  $\nu_3 = \frac{2}{\alpha I_o^3}$ , etc., from Eq. 2. We may remove the DC terms in Eq. 3 by letting

$$v = V - V_o$$

$$\text{and } i = I - I_o.$$

$$\text{Thus, } v = \nu_1 i + \frac{\nu_2}{2!} i^2 + \frac{\nu_3}{3!} i^3 + \dots \quad (4)$$

This equation is of the form of Eq. 1, so this source of third order IM distortion is seen to be caused by the third derivative of the diode I-V characteristic. Thus, if we apply an equal amplitude two-tone current through the diode,

$$i = I \cos \omega_1 t + I \cos \omega_2 t \quad (5),$$

where  $I$  is much smaller than  $I_0$ , then we can find the IM distortion voltage across the diode by substituting Eq. 5 into Eq. 4 and using some trigonometric identities:

$$\begin{aligned} i^3 &= I^3 (\cos^3 \omega_1 t + \cos^3 \omega_2 t + 3 \cos^2 \omega_1 t \cos \omega_2 t \\ &\quad + 3 \cos \omega_1 t \cos^2 \omega_2 t) \\ &= \dots + \frac{3}{4} I^3 \cos (2\omega_2 - \omega_1) t + \dots \end{aligned}$$

$$\text{Thus, } v = \dots + \frac{1}{8} I^3 \nu_3 \cos (2\omega_2 - \omega_1) t + \dots \quad (6)$$

This is the voltage that appears across the diode at one of the third order IM frequencies when the diode is in forward conduction. It can be shown that all four third order IM voltages will have this value.

#### IM IN REVERSE CAPACITANCE

When a Schottky barrier diode is reverse biased it can be modeled as a junction capacitance in parallel with a case capacitance in parallel with a very large resistance to account for leakage current. The junction capacitance  $C_j$  is a function of junction voltage as expressed by

$$C = C_0 \left( \frac{\phi}{V + \phi} \right)^{\gamma} \quad (7),$$

where  $C_0$  is the junction capacitance at zero bias, and  $\phi$  and  $\gamma$  are constants. Again, we assume that the diode is biased by the local oscillator, to some operating point ( $V_0$ ) this time in the reverse region. Now we assume that a small RF voltage is applied across the diode, as shown in Fig. 3. Then we may describe the instantaneous diode capacitance by expanding Eq. 3 in a Taylor series:

$$C = C_0 + k_1(V-V_0) + \frac{k_2}{2!}(V-V_0)^2 + \frac{k_3}{3!}(V-V_0)^3 + \dots \quad (8)$$

where  $k_j = \frac{d^j C}{dV^j}$  evaluated at  $V=V_0$ .

That is,  $k_1 = -\gamma C_0 \phi^\gamma (V_0 + \phi)^{-\gamma-1}$

$k_2 = \gamma(\gamma+1)C_0 \phi^\gamma (V_0 + \phi)^{-\gamma-2}$ , etc.,

from Eq. 7. We remove the DC terms in Eq. 8 by letting

$$c = C - C_0$$

and  $v = V - V_0$ .

Thus,  $c = k_1 v + \frac{k_2}{2!} v^2 + \frac{k_3}{3!} v^3 + \dots \quad (9).$

The charge on this capacitor is found by integrating the capacitance over the voltage, thus

$$\begin{aligned} q &= \int c dv \\ &= \dots + \frac{k_2}{6} v^3 + \dots \end{aligned}$$

The RF current through this capacitor is the time derivative of the capacitor's charge; thus

$$\begin{aligned} i &= \frac{dq}{dt} \\ &= \dots + \frac{k_2}{2} v^2 \frac{dv}{dt} + \dots \end{aligned} \quad (10).$$

This portion of the diode current contains the third order IM current. If we apply an equal amplitude two-tone voltage across the diode such that

$$v = V(\cos \omega_1 t + \cos \omega_2 t) \quad (11),$$

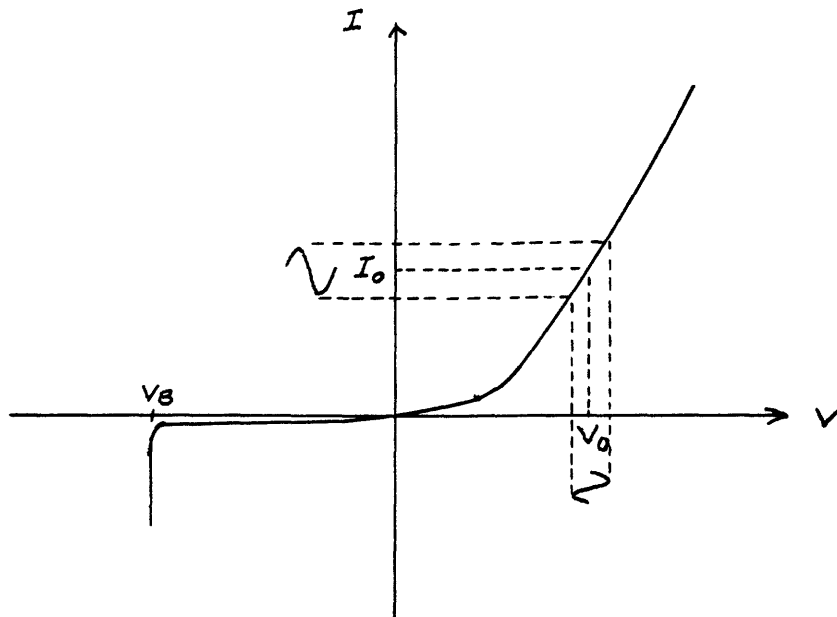


FIG. 2 DIODE CHARACTERISTIC WITH BIAS POINT AND APPLIED RF

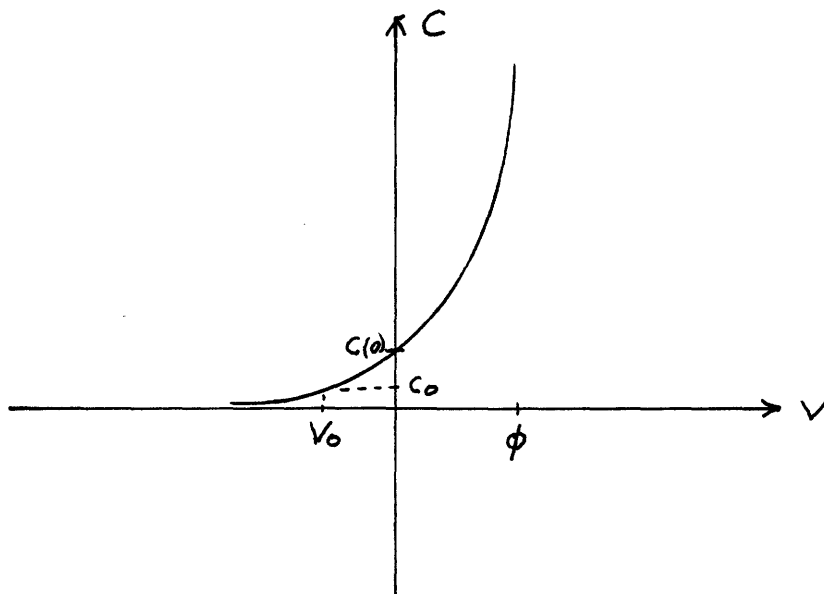


FIG. 3 DIODE CAPACITANCE WITH BIAS POINT

where  $V$  is much smaller than  $V_o$ ,

then  $v^3 = \dots + \frac{3}{4} V^3 \cos (2\omega_1 - \omega_2)t + \dots$ ,

so  $v^2 \frac{dv}{dt} = \frac{1}{3} \frac{d}{dt} (v^3) = \dots - \frac{1}{4} V^3 (2\omega_1 - \omega_2) \sin (2\omega_1 - \omega_2)t$ .

thus  $i = \dots \frac{1}{8} k_2 V^3 (2\omega_1 - \omega_2) \sin (2\omega_1 - \omega_2)t + \dots$  (12)

This term is the third order IM distortion current at the frequency  $2\omega_1 - \omega_2$ . Those at the other third order IM frequencies are of similar form but have different frequency multipliers.

#### IM IN REVERSE CONDUCTION

For diodes biased in the reverse direction but far from the breakdown region (see Fig. 2), the current vs. voltage relationship is approximately that of Eq. 2, with  $V$  and  $I$  negative. This equation is not strictly accurate for Schottky barrier diodes<sup>6</sup>, but it serves as a useful approximation. It can be shown that the IM distortion generated by this source is much smaller than that generated in the junction capacitance for small RF signals, so it can be neglected. When the diode is biased near the breakdown region, however, the reverse leakage current becomes a very non-linear function of the reverse voltage, so a large amount of IM distortion will be generated.

#### IM IN THE TRANSITION REGION

The three sources of IM distortion discussed above have been analyzed on the assumption that the local oscillator

has biased the diodes far enough into the forward or reverse region so that the applied RF signal is a small perturbation about the operating point. This assumption could be valid in a balanced mixer only if a perfect square wave (or some other discontinuous waveform) local oscillator drive were applied. Any real LO drive voltage must have some finite risetime associated with it; thus some percentage of the LO period would be spent with the diodes near zero bias, so that the RF signal across the diodes is comparable to or larger than the bias point produced by the local oscillator.

In this region of operation, IM distortion is generated mainly because of non-linear diode conduction for small reverse bias. If we define  $V$  as the reverse biased diode voltage, then the diode current is

$$I = I_{SAT} (e^{-\alpha V} - 1) \quad (13)$$

where the parameters are defined as in Eq. 2. If we apply a two-tone voltage of amplitude  $V_s$  across the diode, in addition to the small bias voltage  $V_o$ , then  $V$  becomes

$$V = V_o + V_s \cos \omega_1 t + V_s \cos \omega_2 t \quad (14).$$

Substitution into Eq. 13 yields

$$I = I_{SAT} \left( e^{-\alpha V_o} e^{-\alpha V_s \cos \omega_1 t} e^{-\alpha V_s \cos \omega_2 t} - I_{SAT} \right) \quad (15).$$

We may use the following series expansion<sup>7</sup>:

$$e^{z \cos \theta} = I_0(z) + 2 \sum_{k=1}^{\infty} I_k(z) \cos k\theta \quad (16),$$

where the  $I_k$  functions are  $k^{\text{th}}$  order Modified Bessel functions. Applying Eq. 16 to Eq. 15, we find that the diode current at the third order IM frequency  $(2\omega_1 - \omega_2)$  is

$$i_3(t) = 2I_{SAT} e^{-\alpha V_o} I_1(\alpha V_s) I_2(\alpha V_s) \cos(2\omega_1 - \omega_2)t \quad (17).$$



The Modified Bessel functions increase approximately exponentially for large arguments. Thus for large RF signal voltages we may approximate Eq. 17 by the proportionality

$$i_3(t) \propto e^{\alpha(2V_s - V_o)} \cos(2\omega_1 - \omega_2)t.$$

It is seen, then, that in order to make this IM source negligably small, we must make the LO voltage  $V_o$  much larger than the signal voltage  $V_s$ .

#### OTHER SOURCES OF IM

The above described sources of IM are those most immediately apparent from a mixer analysis, and are frequently the most important. Other sources can exist, however, and should be mentioned. A source which is sometimes significant, especially at low frequencies, is the IM distortion generated in the ferrite material frequently used to construct the mixer hybrid transformers. Another source which has been and is being investigated by others<sup>8,9</sup> is the perturbation due to the RF signal on the diode switching waveform.

## THE TWO-STATE ASSUMPTION ON MIXER IM

We have seen in the preceding section that the doubly balanced diode mixer may be modeled as a reversing switch in which switching is accomplished by biasing alternate pairs of diodes in the forward, then the reverse conduction region at the LO rate using a local oscillator. Various sources of IM distortion are seen to arise from this model, mostly due to nonlinearities of the diodes in their various operating regions.

In an effort to derive a simple yet accurate formula for a lower limit on the IM distortion in a balanced mixer, the assumption will be made that only two sources of IM are significant; these are IM due to forward diode nonlinear conduction, and IM due to reverse diode nonlinear capacitance. Before applying this two-state assumption, however, we must determine under what conditions, if ever, it is valid.

It was mentioned earlier that IM in reverse divide conduction can be neglected provided the diode is not operated near breakdown. This can be seen from Eq. 17. Reverse conduction IM is going down exponentially with reverse bias voltage  $V_O$ , whereas reverse capacitance IM is dropping only as  $V_O^{-2}$ , so provided  $V_O$  is large enough, reverse conduction IM will be much smaller than reverse capacitance IM.

Transition IM distortion must be eliminated by using a very rapid risetime square wave LO drive. This will assure that essentially no time is spent in which the diode is operated near zero bias. A corollary condition is that

the RF signal on the diode must be kept small compared to the bias voltage applied by the local oscillator. Note that it is not enough to apply a large sine wave LO drive signal and let the diodes themselves clip this waveform to a square shape; this clipping action does not appreciably affect the LO current, so that appreciable time will be spent in which the forward biased diodes are near zero bias. Then the RF signal will be sufficient to turn these diodes slightly off periodically, producing transition IM distortion.

IM distortion due to ferrite transformers can be readily reduced to negligible levels by using a large volume of ferrite material. IM due to RF perturbation of the switching waveform can be reduced by keeping the RF signal small with respect to the LO drive.

## MIXER IM IN FORWARD BIASED DIODES

The IM distortion in a doubly balanced mixer using the two-state assumption may be more easily analyzed and verified experimentally by breaking up the mixer model into a forward diode circuit and a reverse diode circuit, then combining them by superposition. The forward diode circuit will be treated first; this circuit is shown in Fig. 4. Only one diode is treated at a time, rather than both forward biased diodes at once, so that differences in individual diode nonlinearities may be measured experimentally. The other diode is replaced by a short circuit. The RF signal generator is represented as it looks after being transformed by the input hybrid, as a voltage source  $v_{in}$  and a generator impedance  $R_g$ . The IF load is that transformed through the output hybrid, and is also  $R_g$ . The series resistance of the diode is represented as a constant  $R_s$ . The LO is assumed to provide a constant bias current  $I_0$  through the diode.

If we assume that the RF voltage across the diode junction is small compared to the generator voltage, then the RF current through the diode is

$$i = \frac{1}{2R_g + R_s} v_{in} \quad (18).$$

Then, if we let  $v_{in}$  be a two-tone voltage:

$$v_{in} = V_g (\cos \omega_1 t + \cos \omega_2 t) \quad (19),$$

then we can substitute Eqs. 18 and 19 into Eq. 6 to obtain the third order IM voltage  $v_3(t)$ :

$$v_3(t) = \frac{1}{8(2R_g + R_s)^3} V_g^3 \gamma_3 \cos (2\omega_1 - \omega_2)t \quad (20).$$

Now we can treat the diode as a voltage source of value  $V_3$  and place it in series with the generator voltage source, as in Fig. 5. The third order IM ratio, IMR, which we have defined as the ratio of power dissipated in the output load at one IM frequency, to that at one two-tone frequency, may be computed from this figure. It is

$$\text{IMR} = \frac{1V_3^2}{1V_g^2} \quad (21).$$

$$\text{Thus, IMR} = \frac{1}{64} (2R_g + R_s)^{-6} V_3^2 V_g^4. \quad (22)$$

This expression may be written in terms of the input power of one of the two tones by noting that the power available from the signal generator is

$$P_{in} = \frac{V_g^2}{8R_g} \quad (23).$$

Substituting this expression and the expression for  $V_3$  given earlier, into Eq. 22 we arrive at the final expression for IM ratio due to a single forward biased diode in the circuit of Fig. 4:

$$\text{IMR} = 4 \alpha^{-2} I_o^{-6} (2R_g + R_s)^{-6} R_g^2 P_{in}^2 \quad (24).$$

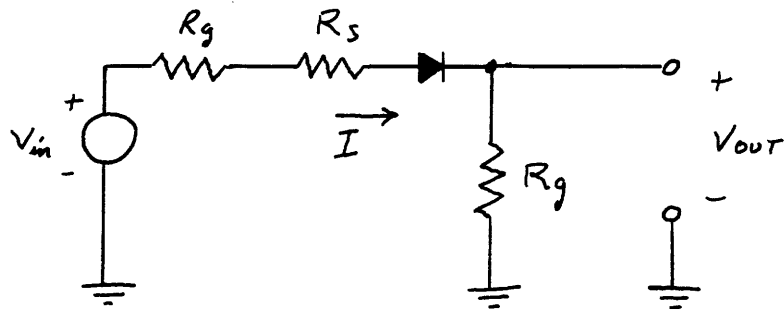


FIG. 4 FORWARD BIASED DIODE SCHEMATIC

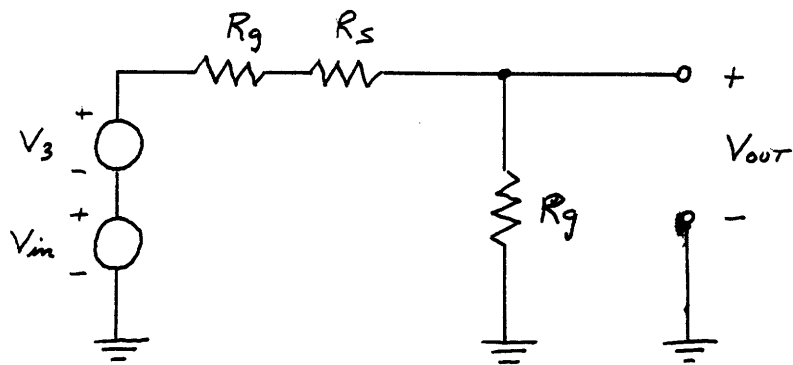


FIG. 5 DIODE REPLACED BY  
IM VOLTAGE SOURCE  $V_3$

## MIXER IM IN REVERSED BIASED DIODES

In the full mixer circuit the diodes that are biased off by the local oscillator appear in shunt across the output load resistor. Thus the circuit shown in Fig. 6 is the appropriate one for computing reverse diode IM distortion. The diode is represented by its nonlinear capacitance. We make the assumption that the diode current is much less than the current flowing through the two resistors  $R_g$ . Then the voltage across the diode may be approximated by

$$V = \frac{V_{in}}{2} \quad (25).$$

If we apply a two-tone input signal by using Eq. 19 again, and substitute this equation and Eq. 25 into Eq. 12 we obtain the diode current at the third order IM frequency  $(2\omega_1 - \omega_2)$ , :

$$i_3(t) = -\frac{1}{64} k_2 V_g^3 (2\omega_1 - \omega_2) \sin (2\omega_1 - \omega_2)t \quad (26).$$

Thus we may treat the diode as a current source of amplitude  $I_3$  as in Fig. 7. The IM ratio is computed by replacing the current source and the output load resistor with their Thevenin equivalent circuit to produce a circuit similar to that of Fig. 5. When this is done the IM ratio is found to be

$$IMR = \left( \frac{1}{64} \right)^2 k_2^2 (2\omega_1 - \omega_2)^2 R_g^2 V_g^4 \quad (27).$$

We may substitute Eq. 23 and the expression obtained previously for  $k_2$  into Eq. 27 to obtain the final expression for third order IM ratio at the frequency  $(2\omega_1 - \omega_2)$  in terms of diode parameters, frequency and input power:

$$IMR = \frac{1}{64} \gamma^2 (\gamma+1)^2 C_o^2 \phi^{2\gamma} (V_o + \phi)^{-2(\gamma+2)} R_g^4 (2\omega_1 - \omega_2)^2 P_{in}^2 \quad (28).$$

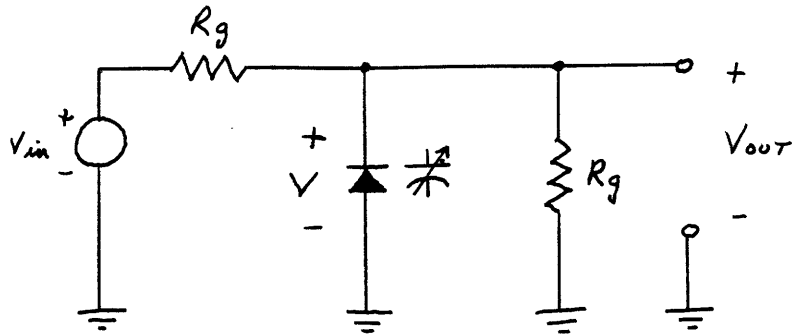


FIG. 6 REVERSED BIASED DIODE SCHEMATIC

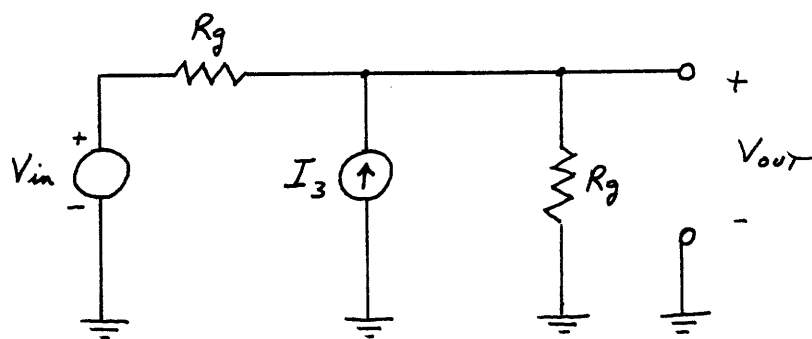


FIG. 7 DIODE REPLACED BY IM CURRENT SOURCE  $I_3$



## TWO-STATE MIXER IM

Now that the IM distortion generated in each diode is known we must combine these sources into a model for the doubly balanced mixer. Fig. 8 shows the evolution of this model. The top diagram is a combination of the circuits of Figs. 5 and 7, with the addition of two opposing diode equivalent sources and their series resistances; this diagram is the equivalent circuit of the mixer during the local oscillator half-cycle when the two horizontal diodes in Fig. 1 are forward biased. The middle diagram in Fig. 8 shows the mixer equivalent circuit during the other LO half-cycle when the two diagonal diodes in Fig. 1 are forward biased. The bottom diagram in Fig. 8 is equivalent to these two circuits when the reversing switch is switched at the LO rate, provided the four diodes are identical, and is thus the IM equivalent circuit of the mixer. Note that both the RF signal generator and the IM distortion generators are on the input of the reversing switch. Thus both the RF signal and the IM distortion are subject to the mixer conversion loss; this means that the IM ratio is independent of the mixer conversion loss.

It must be noted that the addition of these opposing diodes places additional resistors in the single diode circuits of figures 4 through 7. This modifies the expressions for IM ratios  $IMR$ , IM current  $I_3$ , and IM voltage  $V_3$ ; all the  $(2R_g + R_s)$  factors are replaced by  $(2R_g + 2R_s)$ , and all the  $(R_g)$  factors are replaced by  $(R_g + R_s)$ . The result is that the current generators in Fig. 8 are of value

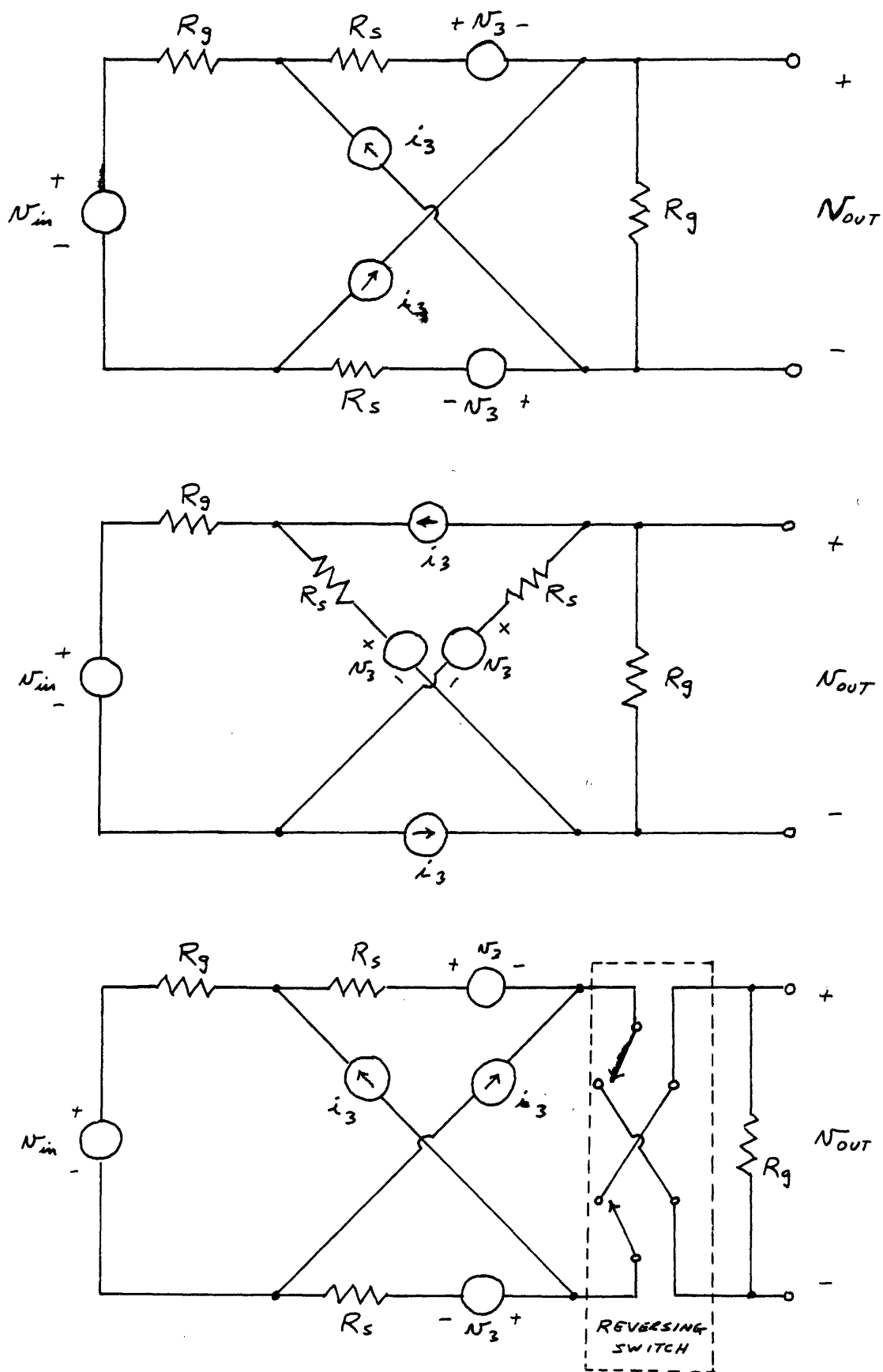


FIG. 8 EVOLUTION OF BALANCED MIXER IM EQUIVALENT CIRCUIT

$$i_3(t) = -\frac{1}{64} k_2 V_g^3 (2\omega_1 - \omega_2) \sin(2\omega_1 - \omega_2)t \quad (29)$$

$$v_3(t) = \frac{1}{64} (R_g + R_s)^{-3} \gamma_3 V_g^3 \cos(2\omega_1 - \omega_2)t \quad (30)$$

$$\text{and } P_{in} = \frac{V_g^2}{8(R_g + R_s)} \quad (31).$$

When the voltages across the IF load resistor due to each source are added by superposition, and when the definition for IM ratio given previously is used, the IM ratio for the mixer is found to be

$$\text{IMR} = \frac{\left| -\frac{R_g}{R_g + R_s} V_3 + R_g I_3 \right|^2}{\left| \frac{R_g}{2(R_g + R_s)} V_g \right|^2} \quad (32).$$

Substituting Eqs. 29 through 31 into Eq. 32, and noting that the cross-product term in the numerator is zero because  $V_3$  and  $I_3$  are orthogonal, the IM ratio becomes

$$\text{IMR} = \frac{1}{16} P_{in}^2 \left[ (R_g + R_s)^{-4} \gamma_3^2 + (R_g + R_s)^4 (2\omega_1 - \omega_2)^2 k_2^2 \right] \quad (33).$$

This expression is the third order IM ratio for the doubly balanced mixer under the two state assumption. Because the mixer effects a frequency shift from input to output the IM ratio is measured as the ratio of IM distortion to desired powers at the translated frequencies. Thus, if the IF frequency

of interest is the difference frequency  $(\omega_s - \omega_{LO})$ , then the IM frequency for which Eq. 33 is valid is  $(2\omega_1 - \omega_2 - \omega_{LO})$ , and the desired frequencies are  $(\omega_1 - \omega_{LO})$  and  $(\omega_2 - \omega_{LO})$ .

Note that the mixer IM ratio is expressed in the form

$$IMR = A (R_g + R_s)^4 + B \frac{1}{(R_g + R_s)^4}.$$

Thus there is an optimum value of generator impedance,

$R_{g \text{ opt}}$  for which this ratio is minimized to some value  $IMR_{\text{opt}}$ .

These optimum values are found by setting the partial derivative of IMR with respect to  $R_g$  in Eq. 33 to zero.

When this is done it is found that

$$R_{g \text{ opt}} = \left[ \frac{\nu_3}{(2\omega_1 - \omega_2)k_2} \right]^{1/4} - R_s \quad (34)$$

$$\text{and } IMR_{\text{opt}} = \frac{1}{8} P_{\text{in}}^2 (2\omega_2 - \omega_1)k_2 \nu_3 \quad (35).$$

## EXPERIMENT

Experimental work was performed to verify the above described theoretical results. DC measurements were made on numerous Schottky barrier diodes to determine the parameters necessary to compute the coefficients  $V_3$  and  $k_2$ . Mixers operating at several generator impedances were constructed with provision for plugging the diodes into each one. These mixers were then used to measure third order IM ratios for single diodes in forward and reverse bias, and for doubly balanced mixers themselves. Given below is a detailed description of each experimental procedure, followed by the results of these experiments and their comparison with theory.

### DIODE PARAMETER MEASUREMENTS

The current through a forward biased Schottky barrier diode is the same as in Eq. 13. The diode also possess a series resistance  $R_s$  which will have an additional voltage across it

$$V_s = R_s I \quad (37).$$

Thus we may write an expression for the diode current in terms of the voltage drop across the entire diode,  $V_D = V + V_s$ , as

$$I = I_{SAT} (e^{\alpha (V_D - R_s I)} - 1) \quad (38).$$

For fairly large diode voltages this may be approximated as

$$I = I_{SAT} e^{\alpha (V_D - R_s I)} \quad (39),$$

$$\text{so } \log I = \log I_{\text{SAT}} + \alpha (V_D - R_S I) \log e \quad (40)$$

Thus if  $\log I$  were plotted vs.  $V_D$ , the result would be a straight line of slope  $\alpha \log e$  wherever  $V_D$  was large enough to make  $e^{\alpha V_D} \gg 1$  and  $I$  was small enough to make  $R_S I \ll V_D$ . If extended to the  $I$  axis this straight line would intersect at  $I = I_{\text{SAT}}$ . So two diode parameters,  $\alpha$  and  $I_{\text{SAT}}$ , can be determined.

If this straight line were extended above the point at which it departs from the plotted data, the voltage difference  $\Delta V$  between this line and the data would be

$$\Delta V = V_D - V = R_S I \quad (41).$$

Thus, a plot of  $\Delta V$  vs.  $I$  would be a straight line of slope  $R_S$ , provided  $R_S$  is constant. In this way the diode series resistance  $R_S$  may be determined.

The junction capacitance  $C$  of a reverse biased Schottky diode is given in Eq. 7. The total diode capacitance  $C_D$  is the junction capacitance in parallel with a case capacitance  $C_{\text{case}}$ . Thus  $C_D = C_o \left( \frac{\phi}{V + \phi} \right)^{\gamma} + C_{\text{case}}$  (42).

In this case  $V$  may be considered the diode voltage  $V_D$  since the voltage drop across the series resistance is negligible in the reverse biased diode.

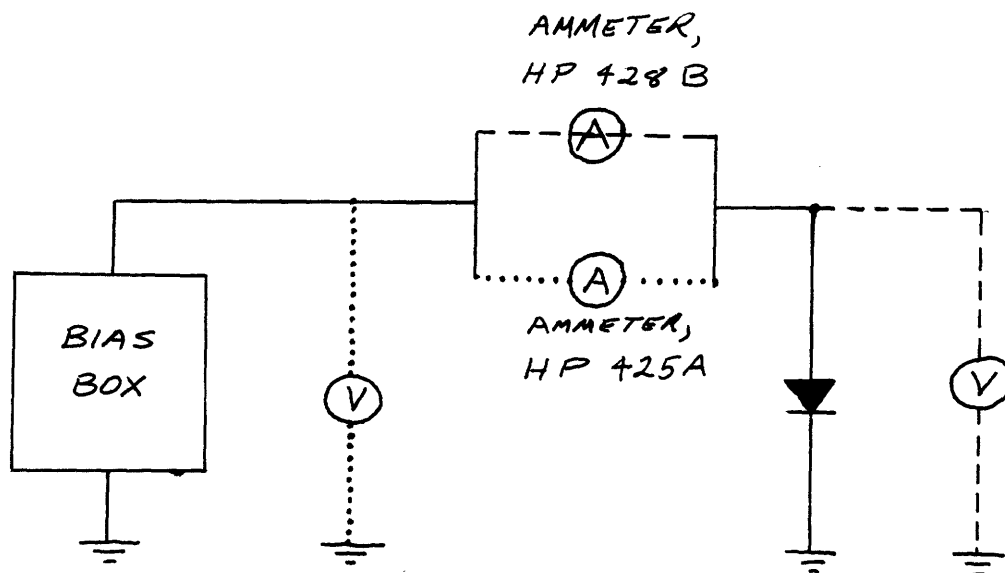
A computer program has been devised and written<sup>10</sup> which fits data of diode capacity vs. voltage in a best mean square manner to Eq. 42. This program thus determines the coefficients  $C_o$ ,  $\phi$ ,  $C_{\text{case}}$ , and  $\gamma$  which simultaneously best fit the data.

The experimental set-up used to measure the diode conduction parameters  $I_{SAT}$ ,  $\alpha$  and  $R_s$  is shown in block diagram form in Fig. 9. The dotted lines show connections for low current measurements (less than 1 ma), and the dashed lines show connections for higher current measurements (between 1 and 50 ma). The bias box is simply a battery with variable resistive voltage divider and variable series resistance.

Measurements of diode capacitances were made with a Boonton Electronics capacitance bridge. This bridge has internal DC isolation for test device biasing and measures capacitance to a precision of .0001 picofarads. Extremely careful measurements must be made of diode capacitance because the computer program is very sensitive to errors and is only accurate when at least twenty data points are given.

The results of forward conduction measurements of several Schottky diodes are shown graphically in Figs. 10 and 11. Only one diode of each type is shown in these figures. Measurements were made on four matched diodes of each type, but the curves of  $\log I$  vs.  $V$  and  $I$  vs.  $\Delta V$  are so similar for the matched diodes that they overlap. The diodes used were Solitron type MSQ5140, HP Associates type HP2301, and Solitron type MSQ7330 silicon Schottky barrier diodes.

Note that the slope of the  $I$  vs.  $\Delta V$  curve is constant up to a certain value of  $I$  for the MSQ5140 and HP2301 diodes, then changes beyond this current. This change in the slope (ie change in  $R_s$ ) is likely due to diode heating at the higher current levels; the series resistance is dependent on carrier mobility in the semiconductor material, which is temperature



V : DIGITAL VOLTMETER,  
HP 3440A

FIG. 9 FORWARD BIASED DIODE  
PARAMETER MEASUREMENT SET-UP



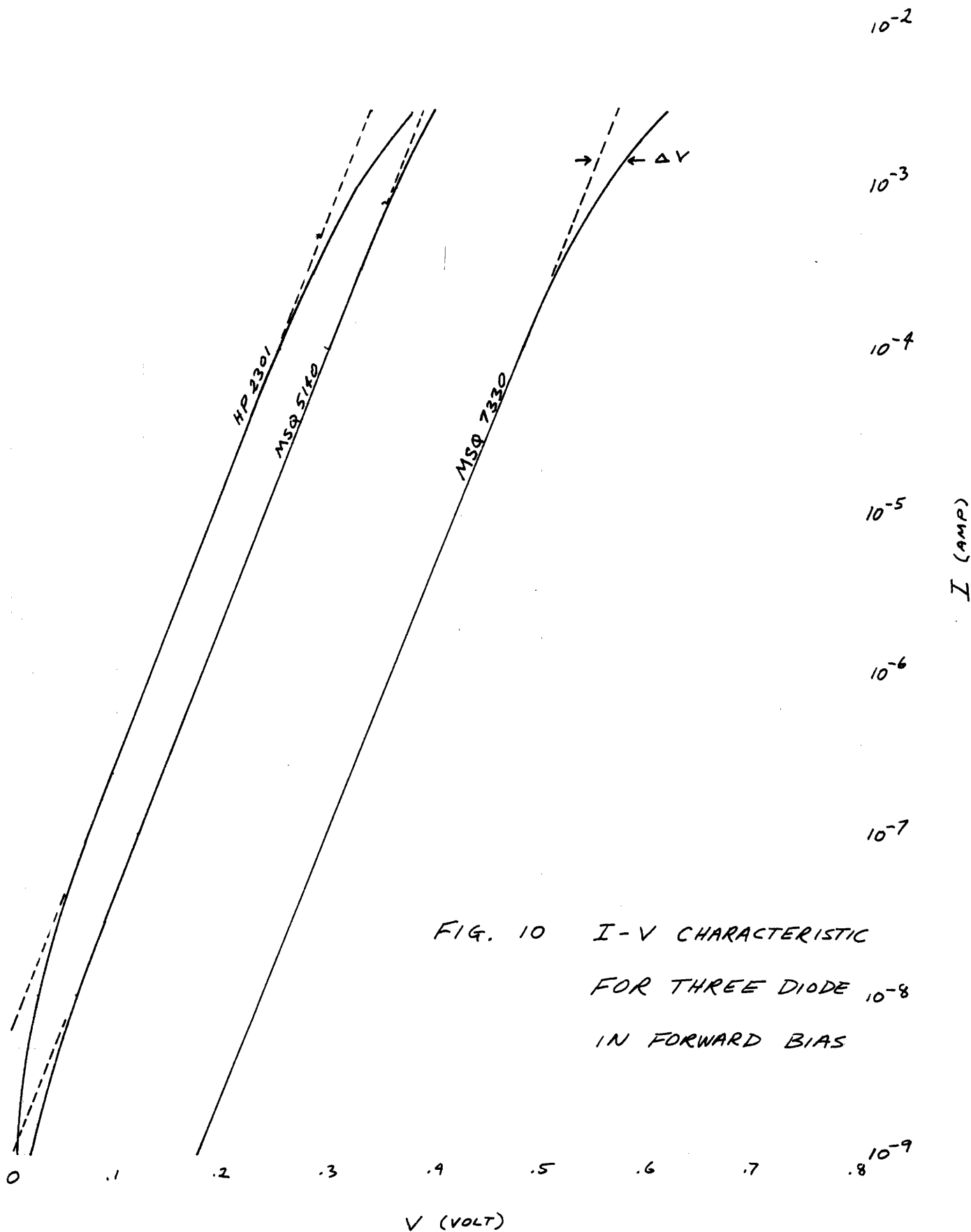


FIG. 10 I-V CHARACTERISTIC  
FOR THREE DIODE  $10^{-8}$   
IN FORWARD BIAS

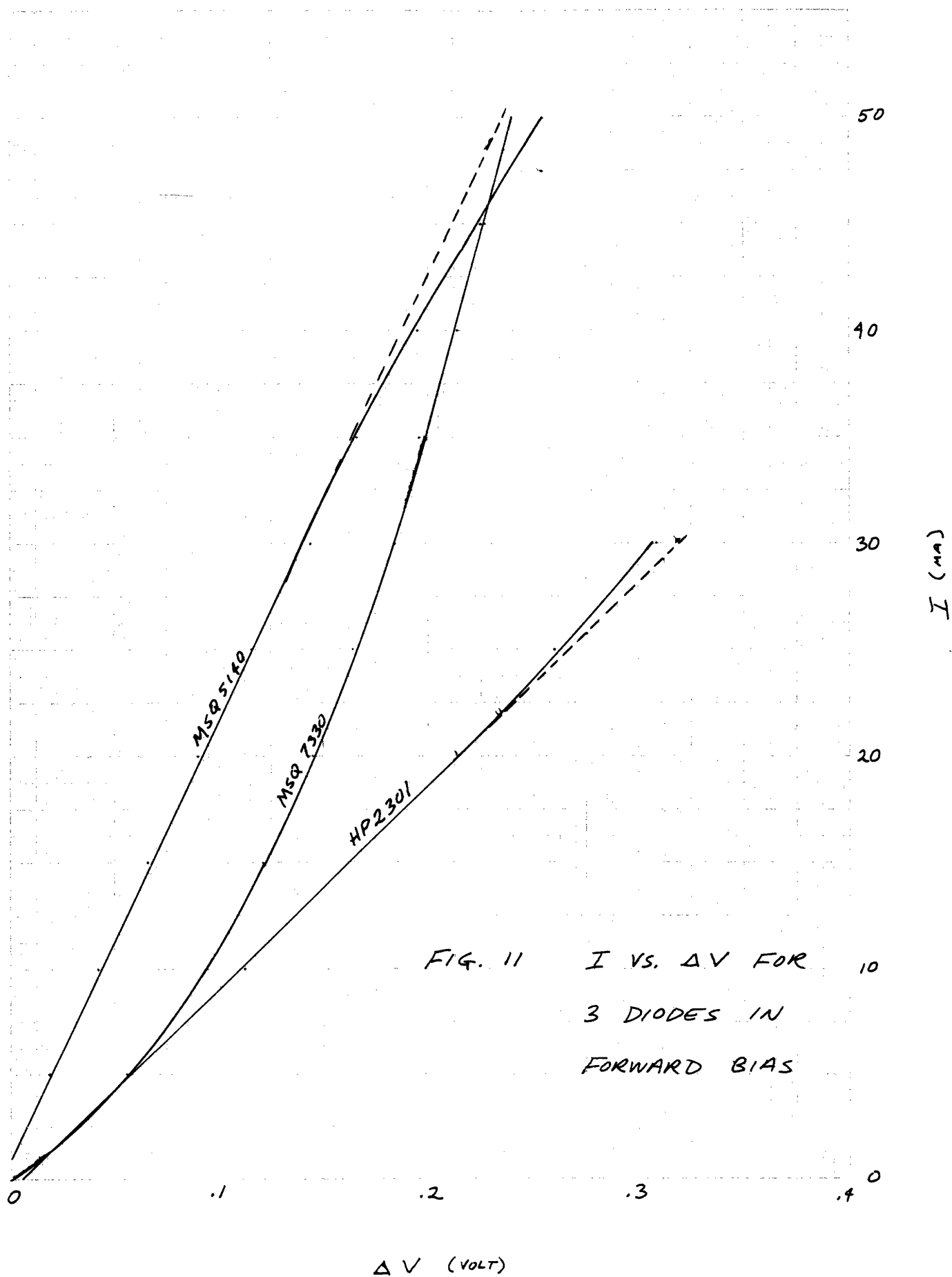


FIG. 11  $I$  VS.  $\Delta V$  FOR 10  
3 DIODES IN  
FORWARD BIAS

dependent. The  $I$  vs.  $\Delta V$  curve for the MSQ7330 diode is more nonlinear than the others, however; this may be due to some minority carrier current flow in addition to the heating effect. Minority carrier current can cause conductivity modulation, ie a change of conduction with current. Minority carrier current is detrimental to the diode's operation because it decreases the switching speed of the diode.

The diode parameters which have been computed from graphs such as Figs. 10 and 11, and those which have been computed using the computer program, are tabulated for each diode in Table 1. The series resistance given for the MSQ7330 diode is arbitrarily measured at 10 ma; that for the other diodes is measured at low current.

TABLE 1

## DIODE DC PARAMETERS

Diode	$I_{SAT}$ (amp)	$\alpha$ (volt <sup>-1</sup> )	$R_s$ (ohm)	$C_o$ (pf)	$\phi$ (volt)	$\gamma$
MSQ 5140-1	$1.2 \times 10^{-9}$	38.0	4.94	.331	.38	.51
MSQ 5140-2	$1.3 \times 10^{-9}$	37.9	5.00	.343	.37	.48
MSQ 5140-3	$1.2 \times 10^{-9}$	38.9	4.95	.343	.41	.54
MSQ 5140-4	$1.1 \times 10^{-9}$	39.1	4.90	.361	.37	.47
MSQ 7330	$1.2 \times 10^{-12}$	37.6	6.20			
HP 2301	$5.6 \times 10^{-9}$	38.7	8.60			

## TEST MIXER CONSTRUCTION AND PERFORMANCE

Three test mixers were constructed in which to test the Schottky diodes for IM distortion. These mixers have input and output hybrid transformers which convert the 50 ohm unbalanced generator and load impedance to 50 ohms balanced for the first mixer, 100 ohms balanced for the second, and 200 ohms balanced for the third; refer to Fig. 1 for the generalized mixer schematic.

Several requirements had to be met in designing these mixers. The hybrids had to have low loss and low VSWR over as large a bandwidth as possible, in order to come as close to the ideal broad-band mixer structure as possible. The output impedance had to be well balanced about the center tap and the ground plane to assure that the diodes were driven symmetrically. Finally, there had to be some means of changing the diode quad from one mixer to the next without changing the diodes' positions with respect to themselves or the ground plane; such a change would introduce unwanted variables in the experiment.

The design requirements for the hybrids were met by using transmission line transformers.<sup>11</sup> These transformers are capable of low loss, low VSWR and excellent balance over multi-decade bandwidths when carefully constructed.

The diodes are made easily interchangeable from mixer to mixer by building each mixer, less the diodes, as a test fixture. The outputs of the hybrids are fed through

four coaxial lines, of appropriate impedance, to a set of four subminiature OSSM coaxial connectors. The diodes are mounted on a small board on which are four OSSM connectors; these mate with the connectors on the mixer fixture to form a complete mixer. To change the diodes from one mixer to another it is only necessary to disconnect these four connectors.

The three mixer test fixtures are shown schematically in Figs. 12 through 14. Note that the local oscillator is fed to the hybrid center-taps through a 50 ohm unbalanced to 50 ohm balanced transformer in all three mixers.

These mixer fixtures performed satisfactorily from 2 MHz to beyond 300 MHz, which was the maximum frequency at which they were tested. Measurements on the fixtures themselves were made by replacing the diode board with a board consisting of two open circuits and two short circuits. In this way the loss through the fixtures was found to be less than 2 db with a VSWR of less than 1.5 over the 2 to 300 MHz bandwidth. Balance was measured by injecting a signal in the LO port and measuring the leakage power out the RF and IF ports. Ideally the leakage will be zero; these mixers had leakage power more than 50 db below the input available power.

A local oscillator was required that would produce a good square wave at the LO frequency. The circuit used is shown in Fig. 16 and consisted simply of two step recovery diodes back to back, followed by a 300 MHz bandwidth amplifier, and attenuators to reduce the source VSWR.

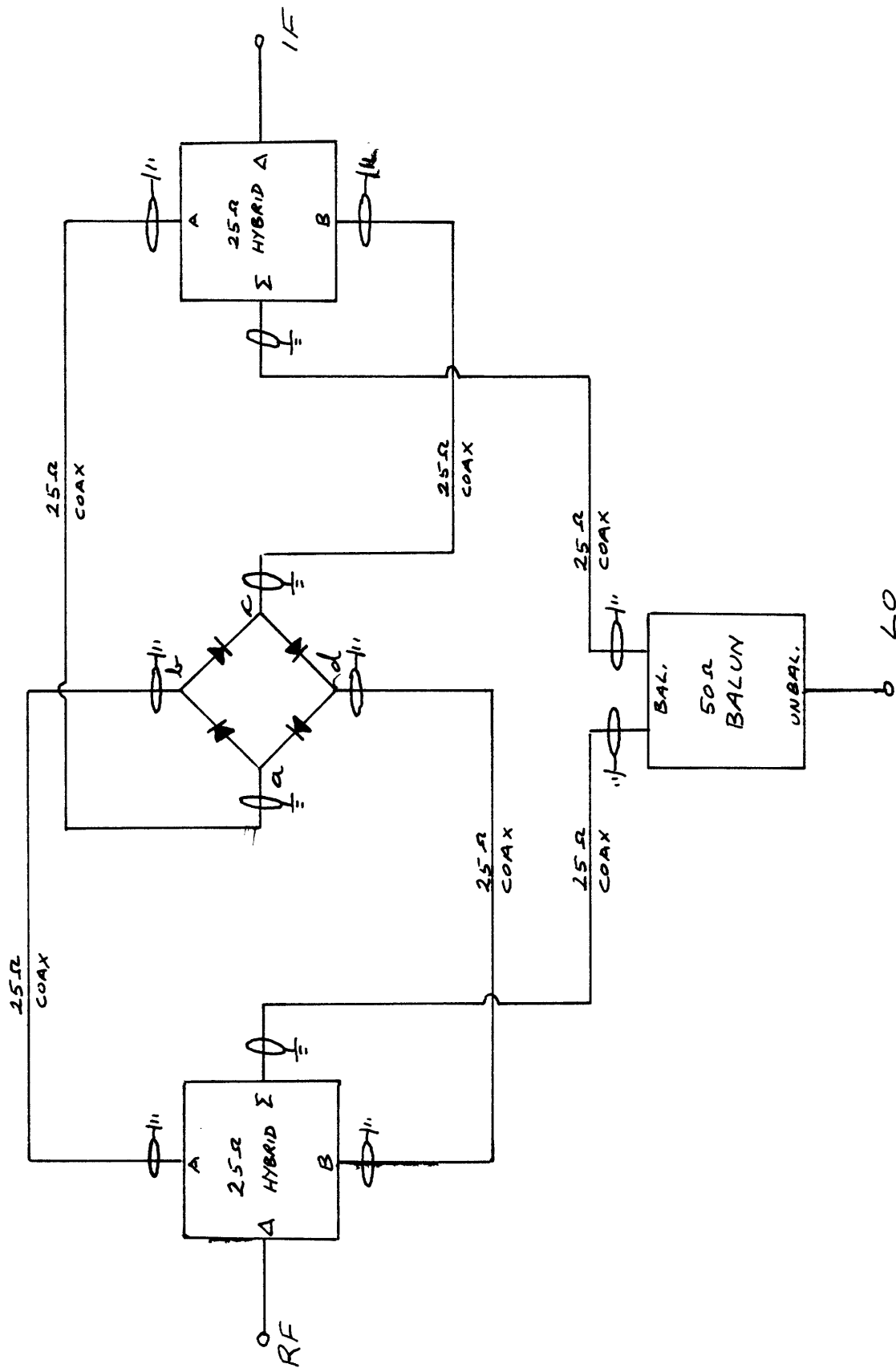


FIG. 12 50 OHM MIXER SCHEMATIC

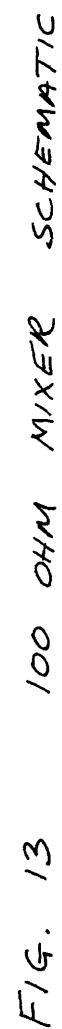






FIG. 14 200 OHM MIXER SCHEMATIC



Room 14-0551  
77 Massachusetts Avenue  
Cambridge, MA 02139  
Ph: 617.253.5668 Fax: 617.253.1690  
Email: docs@mit.edu  
<http://libraries.mit.edu/docs>

## **DISCLAIMER OF QUALITY**

Due to the condition of the original material, there are unavoidable flaws in this reproduction. We have made every effort possible to provide you with the best copy available. If you are dissatisfied with this product and find it unusable, please contact Document Services as soon as possible.

Thank you.

**Pages are missing from the original document.**

*Pg. 42 does not exist*

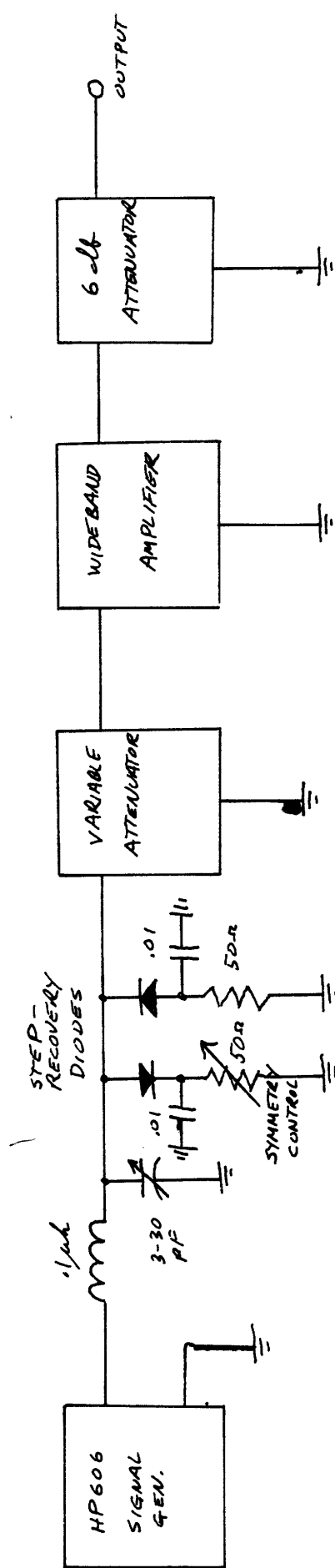
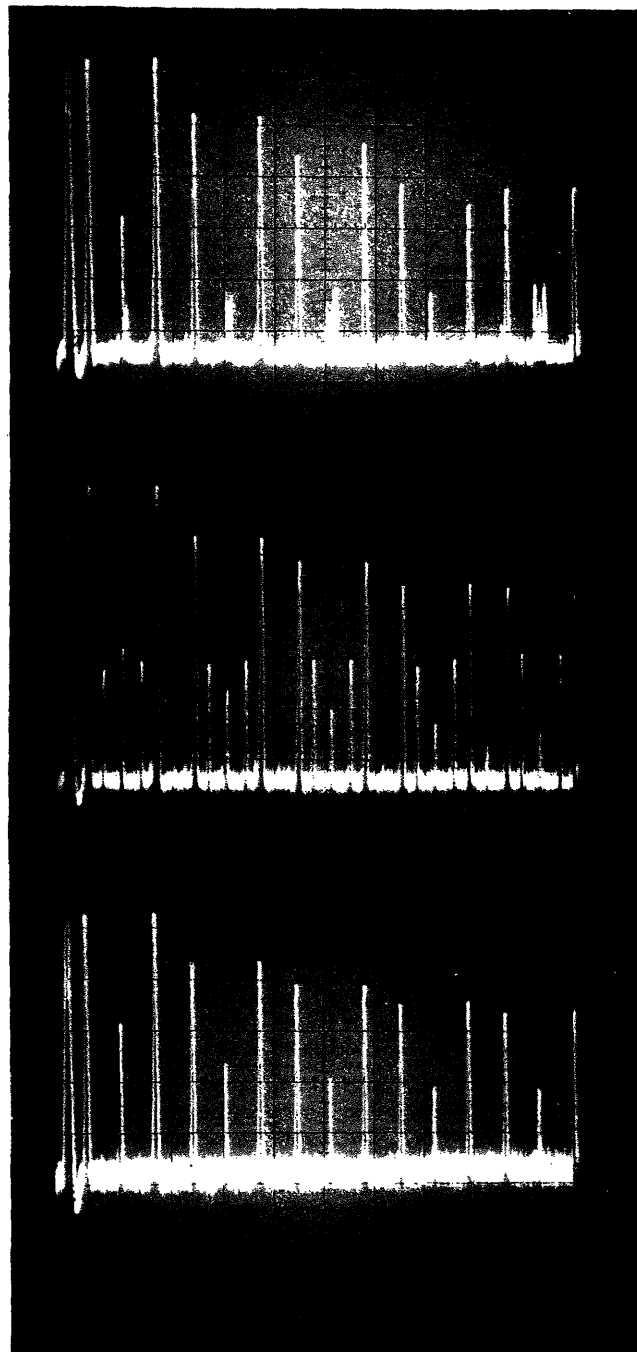


FIG. 16 SQUARE WAVE LOCAL OSCILLATOR

The diodes were driven by a 200 mw sine wave at the LO frequency. The diodes were self biased and a pot was provided to make the waveform symmetrical.

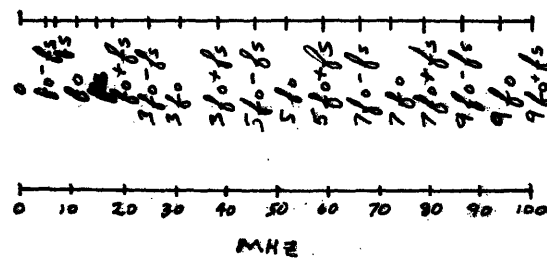
Typical mixer output spectra are shown in Fig. 17. These are taken using the MSQ5140 diodes in the 50 ohm mixer fixture. In all three spectra the signal and LO frequencies are approximately 7 and 10 MHz, respectively. The top spectrum is taken using a sine wave local oscillator. Note that the ratios of high odd-order mixing products are far from those predicted by mixer theory. See Table 2. The middle spectrum is taken using the square wave generator with a 1 per cent asymmetry in its waveform. Note that this asymmetry produces a series of signals all approximately 34 db below the IF frequencies  $f_o \pm f_s$ . These correspond to mixing products of even harmonics of the LO and arise because of the train of narrow pulses which represent the LO asymmetry. In the bottom spectrum these signals have been eliminated by adjusting the symmetry control on the square wave generator. Note also that the ratios of high odd-order mixing products are very close to those of the ideal doubly balanced mixer, as shown in Table 2. The local oscillator feedthrough signal and its odd-order harmonics are not quite in the proper ratio for a square wave, however, indicating that the waveform of the local oscillator is not perfectly square. The mixer conversion loss was observed to be 6 db for both sine and square wave LO drives.



SINE WAVE  
LO

UNSYMMETRICAL  
SQUARE WAVE  
LO

SQUARE WAVE  
LO



VERT. SCALE:  
10db/cm

FIG 17 MIXER OUTPUT SPECTRA

TABLE 2

## BALANCED MIXER SPECTRUM

Given below are power ratios in db of the mixing products of the form  $nf_{LO} \pm f_s$ , (where n is odd,  $f_{LO}$  and  $f_s$  are the LO and signal frequencies respectively) to the power at the IF,  $f_{LO} \pm f_s$ :

	Ideal Mixer	50 ohm mixer with sine wave LO drive (+, -)	50 ohm mixer with square wave LO drive
$3f_{LO} \pm f_s$	9.6 db	11.0, 11.0 db	9.5 db
$5f_{LO} \pm f_s$	14.0	16.5, 18.5	14.0
$7f_{LO} \pm f_s$	16.8	28.0, 24.5	17.5
$9f_{LO} \pm f_s$	19.0	25.0, 24.5	20.0
conversion loss (SSB)	3.9	6.0	6.0

## MEASUREMENT OF IM DISTORTION

An experimental verification of the IM theory requires that some means is available to measure IM distortion. A convenient instrument for this purpose would be a spectrum analyzer because the appropriate IM signal could be found quickly from its relationships with other signals, and the IM ratio could be determined directly from the display scope. Unfortunately, commercially available spectrum analyzers produce IM distortion of their own which is often much greater than that being measured. Some means must be found to eliminate the high-power two-tone signals as they enter the spectrum analyzer, without disturbing the distortion signals. Filters could be used, of course, but then changing frequencies would necessitate changing filters.

A feedforward scheme was used to cancel the two-tone signals as they entered the spectrum analyzer. The setup used to measure IM ratio in single diodes is shown in Fig. 18. Signal generators 1 and 2 generate the two-tone signal, which is combined in hybrid 3 and fed into the device under test. Each tone is also fed into a reference arm by hybrids 1 and 2, and combined in hybrid 4. The output of the test device contains the two-tone signal plus distortion signals. This output is combined with the reference two-tone from hybrid 4, in hybrid 5. By making the time delays in the test arm and two reference arms equal, and by adjusting attenuators to make the reference and test device two-tone amplitudes equal,

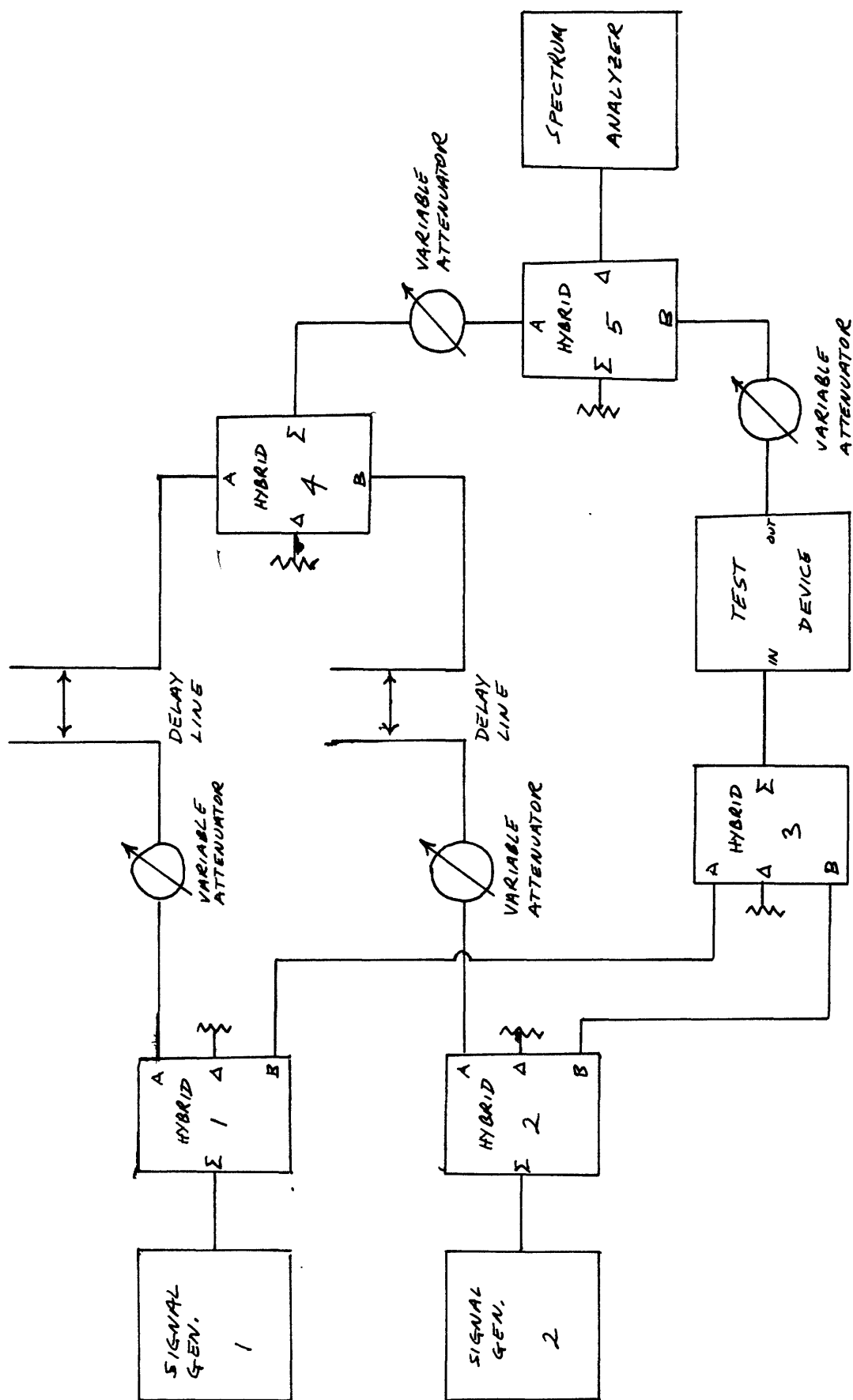


FIG. 18 SINGLE DIODE IM MEASUREMENT SET-UP



these two-tones are made to cancel each other in hybrid 5, leaving only the distortion signals to be fed into the spectrum analyzer, after being amplified.

In operation, this feedforward setup can be tuned to produce more than 80 db of two-tone cancellation. This is sufficient to keep spectrum analyzer IM distortion below -140 dbm, the sensitivity of the analyzer plus pre-amplifier, for input two-tone levels under +20 dbm. The dynamic range of the system is limited by the amount of IM distortion generated in the signal generators due to imperfect isolation in hybrid 3 and possibly through the generator power lines. The system dynamic range is measured in the setup of figure 18 by replacing the test device with a length of transmission line and measuring the IM ratio on the spectrum analyzer after tuning up the system. This system had a third order IM ratio of -127 db for a +13 dbm two-tone signal at the test device input for frequencies above approximately 4 MHz.

A similar system can be constructed in principle to measure IM distortion in mixers, by simply placing a mixer in each reference arm and driving all three mixers with a single local oscillator. The problem here is that many signals appear at the mixer outputs, and all must be canceled simultaneously. Thus three very closely matched mixers are required. The system finally used was that shown in Fig. 19, which consists simply of a 30 MHz band-pass filter, with a 10 db pad to absorb reflected power, in front of the spectrum analyzer. The signal and LO frequencies were selected to place one of the third order IM signals at 30 MHz; all other signals were then filtered

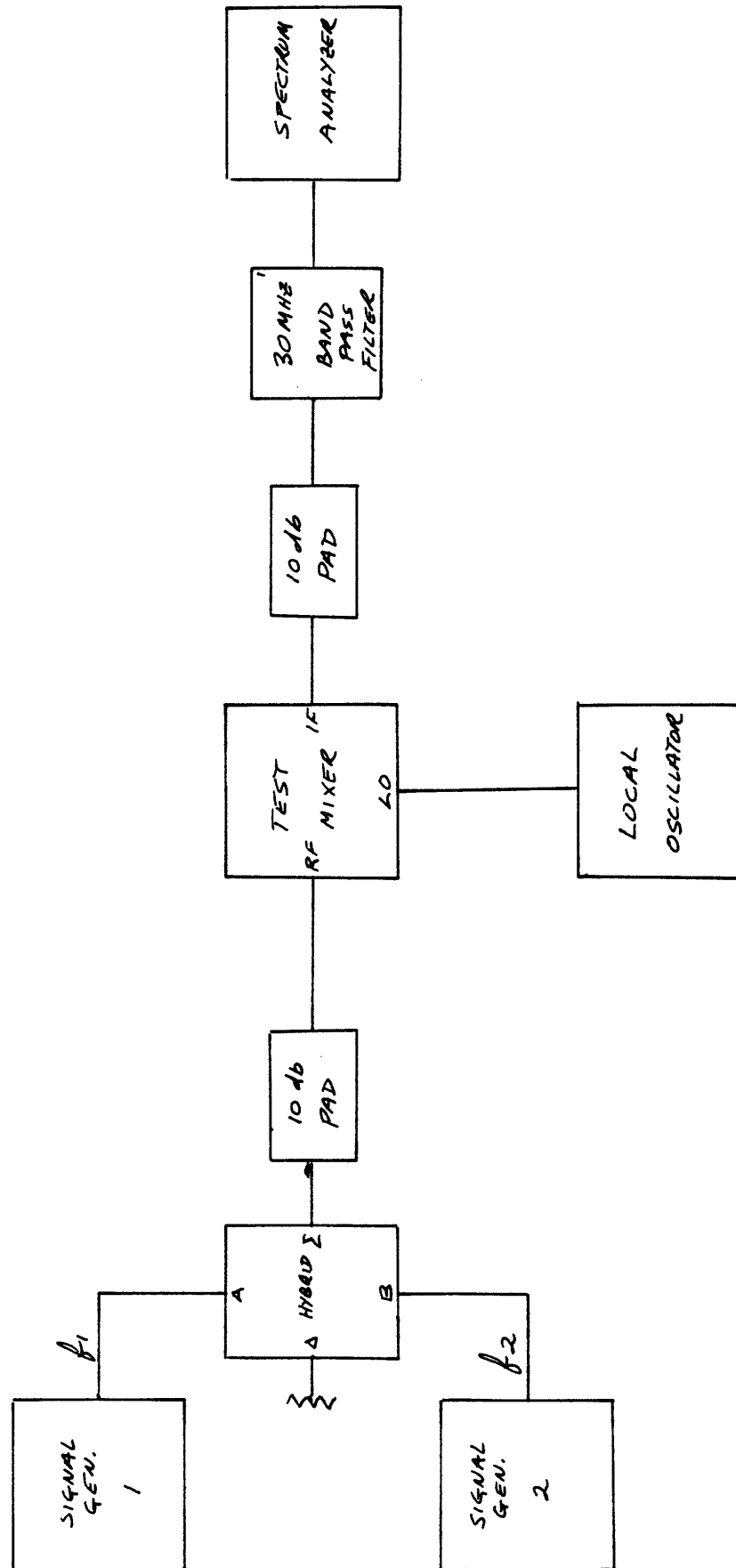


FIG. 19 MIXER IN MEASUREMENT SET-UP

out. In making these measurements the frequencies must be changed so that both the IM signals surrounding the IF can be measured to insure that they are equal amplitude.

## IM RATIO IN DIODES

The mixer test fixtures were used to measure the IM ratios of forward and reverse biased diodes in the circuits of Figs. 4 and 6. A diode test board was wired as shown in Fig. 20 for the forward diode measurements, and as shown in Fig. 21 for the reverse diode measurements. Bias was applied through the RF choke shown. The IM ratios were measured using the setup of Fig. 18.

The results of these measurements are shown graphically in Figs. 22 through 32. These measurements are compared with the theoretical predictions as derived previously; the theoretical curves are plotted as dotted lines. There are experimental errors in both the experimental and theoretical data plotted here. The experimental data is subject to input power measurement error and errors in measuring the IM ratio on the spectrum analyzer. These result in an estimated  $\pm 3$  db possible error in the experimental data. The possible error in the theoretical curves are due to diode parameter measurement errors, since these parameters are used to compute the theoretical IM ratios. The forward biased diode parameters,  $\alpha$  and  $R_s$ , are measured directly and may be assumed to be fairly accurate. Reference to Eq. 24 shows that these parameters are not heavily weighted factors in the IM ratio expression. Thus the possible error in the theoretical curves for the forward biased diodes will be small, i.e. less than  $\pm 1$  db. The reverse diode parameters are indirectly found from diode measurements, since a computer computation is involved. Thus these parameters are not so accurately

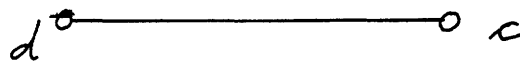
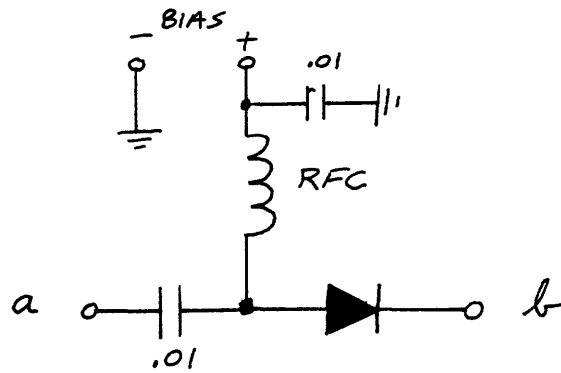


FIG. 20 FORWARD-BIASED DIODE  
TEST BOARD SCHEMATIC

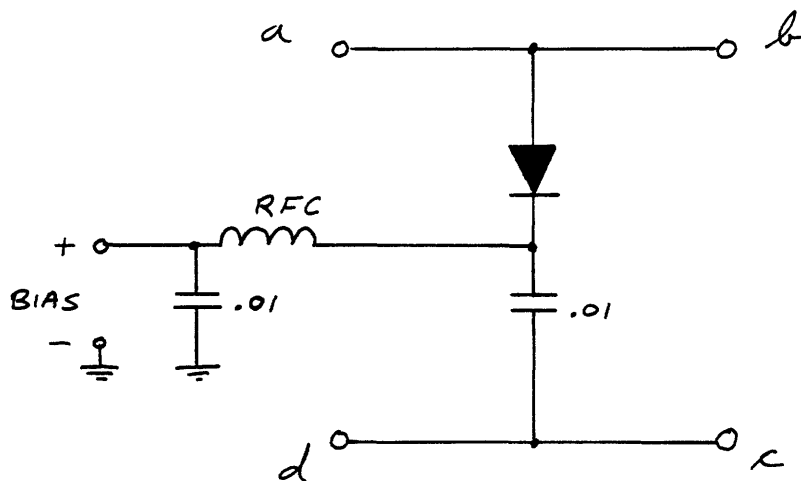


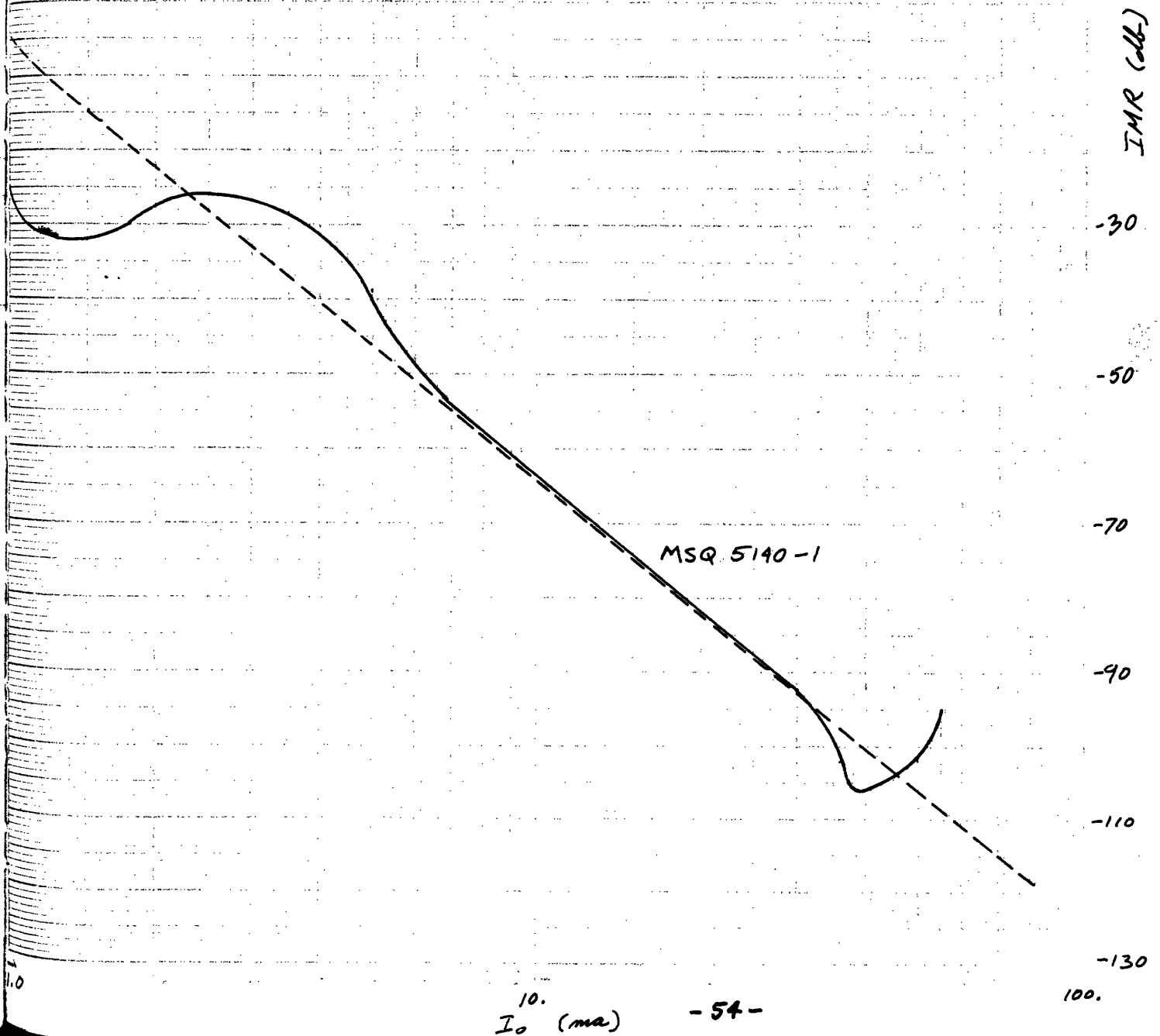
FIG. 21 REVERSE-BIASED DIODE  
TEST BOARD SCHEMATIC

$f_1 = 30 \text{ MHz}$   
 $f_2 = 32 \text{ MHz}$   
 $P_{in} = -6 \text{ dbm}$   
 $R_g = 50 \Omega$

FIG. 23 a.

IMR VS. FORWARD  
BIAS CURRENT

MSQ 5140 DIODE



$$f_1 = 30 \text{ MHz}$$

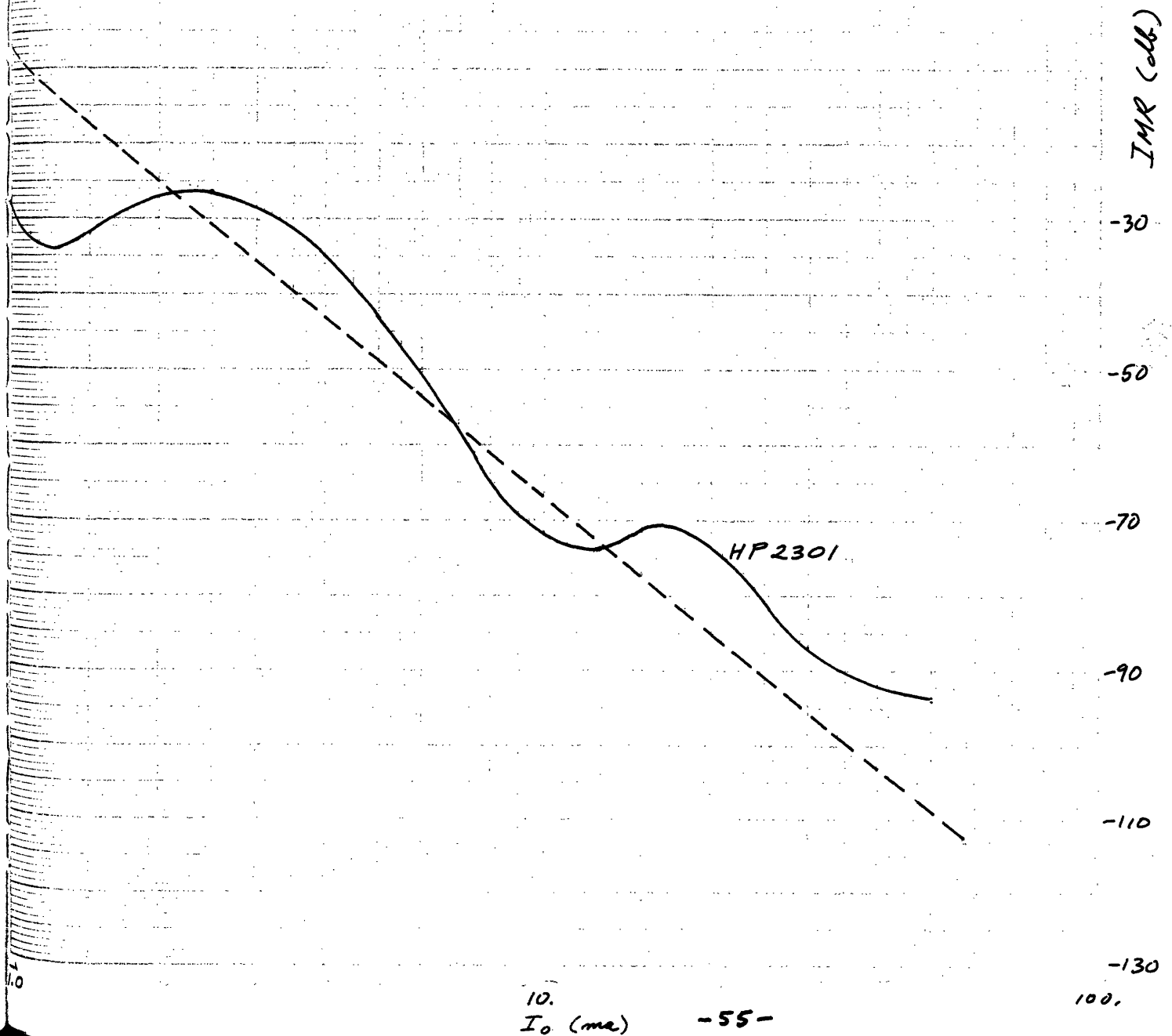
$$f_2 = 32 \text{ MHz}$$

$$P_{in} = -6 \text{ dbm}$$

$$R_g = 50 \Omega$$

FIG. 22 b. IMR VS. FORWARD  
BIAS CURRENT

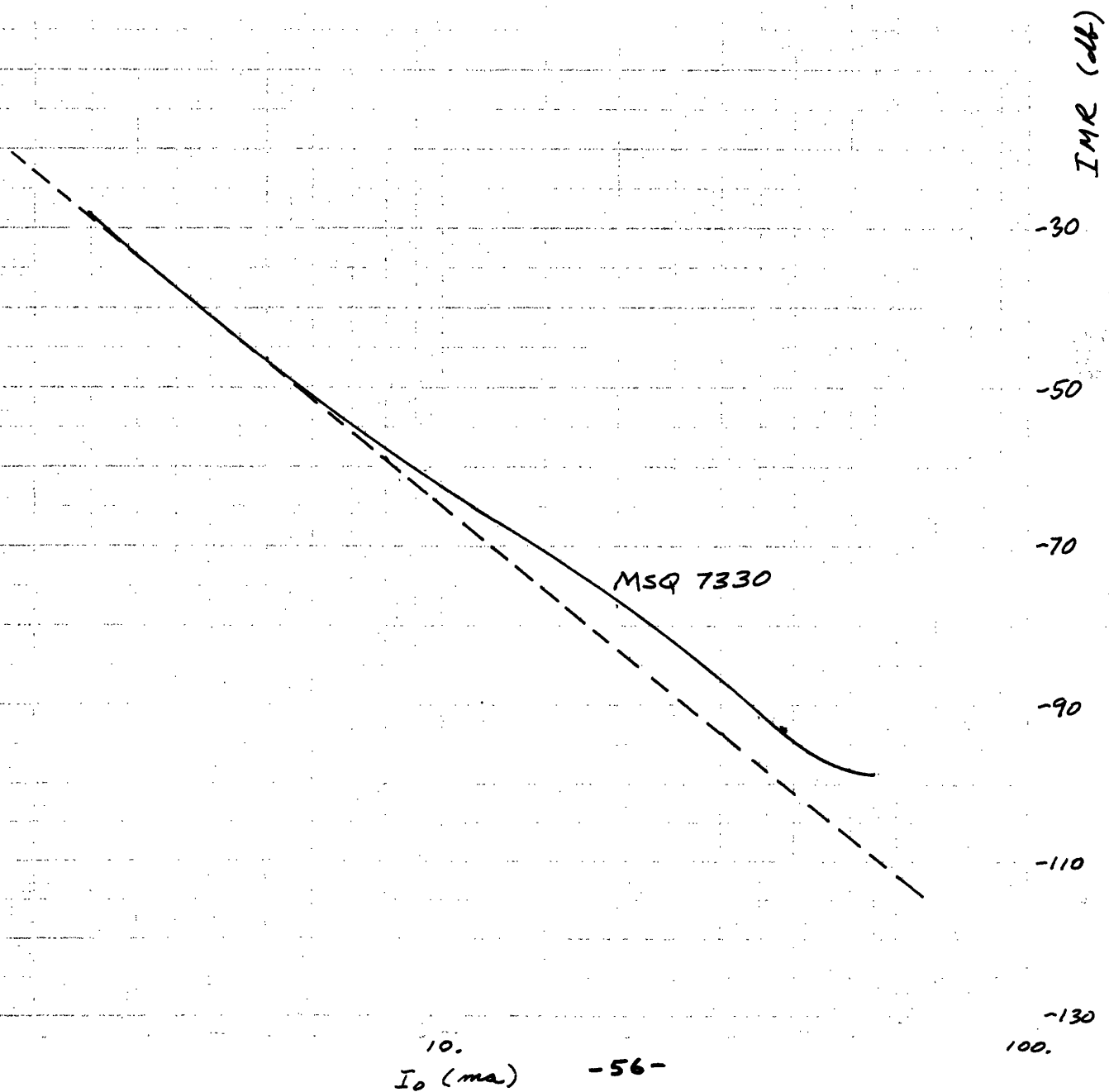
HP 2301 DIODE



$f_1 = 30 \text{ MHz}$   
 $f_2 = 32 \text{ MHz}$   
 $P_{in} = -6 \text{ dbm}$   
 $R_g = 50 \Omega$

FIG. 22 c. IMR VS. FORWARD  
BIAS CURRENT

MSQ 7330 DIODE





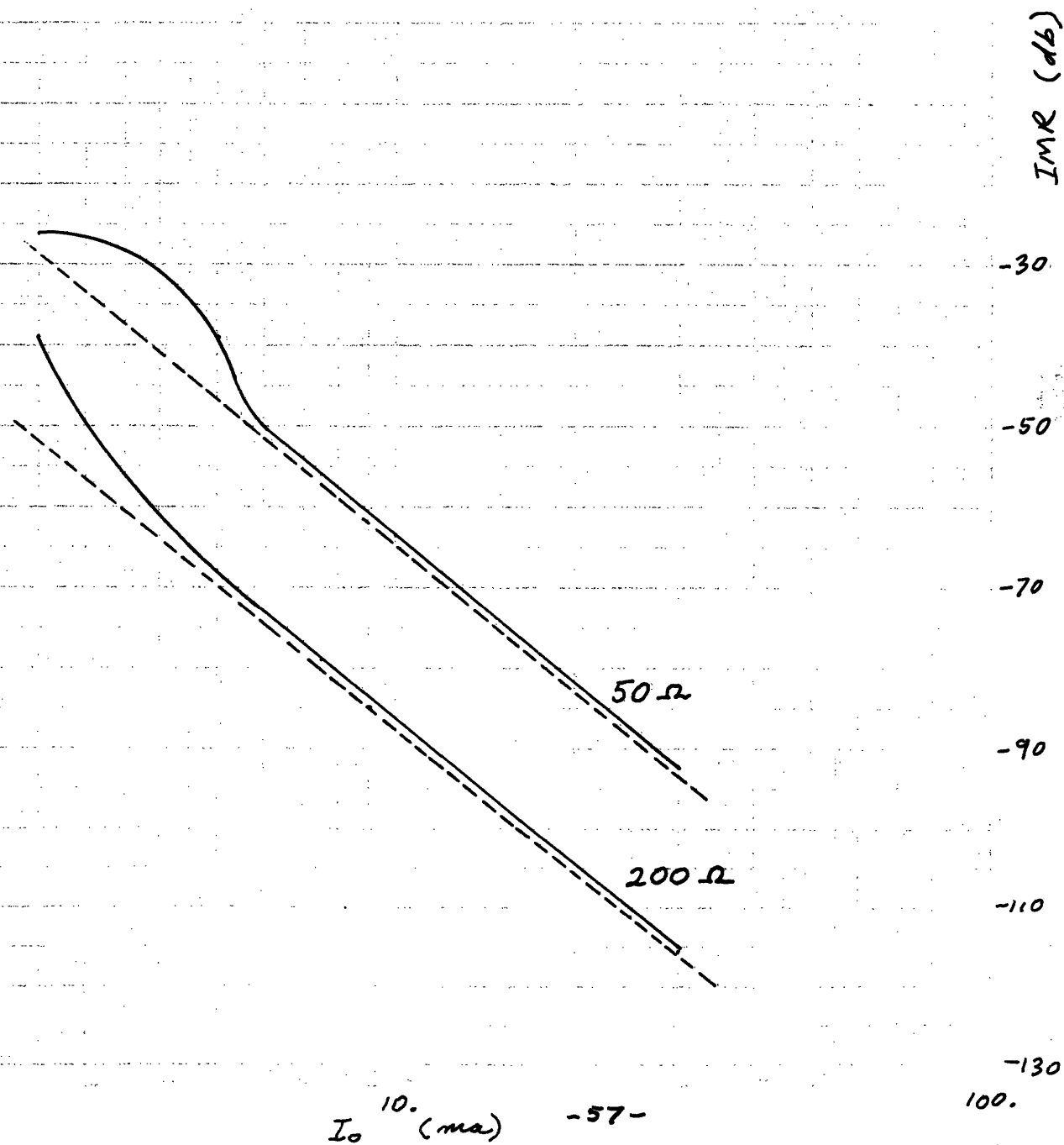
MSQ 5140-1

$f_1 = 30 \text{ MHz}$   
 $f_2 = 32 \text{ MHz}$

$P_{in} = -6 \text{ dbm}$

FIG. 23 IMR VS. FORWARD  
BIAS CURRENT  
AND SOURCE IMPEDANCE

DIODE 1



$I_0$  10. (ma)

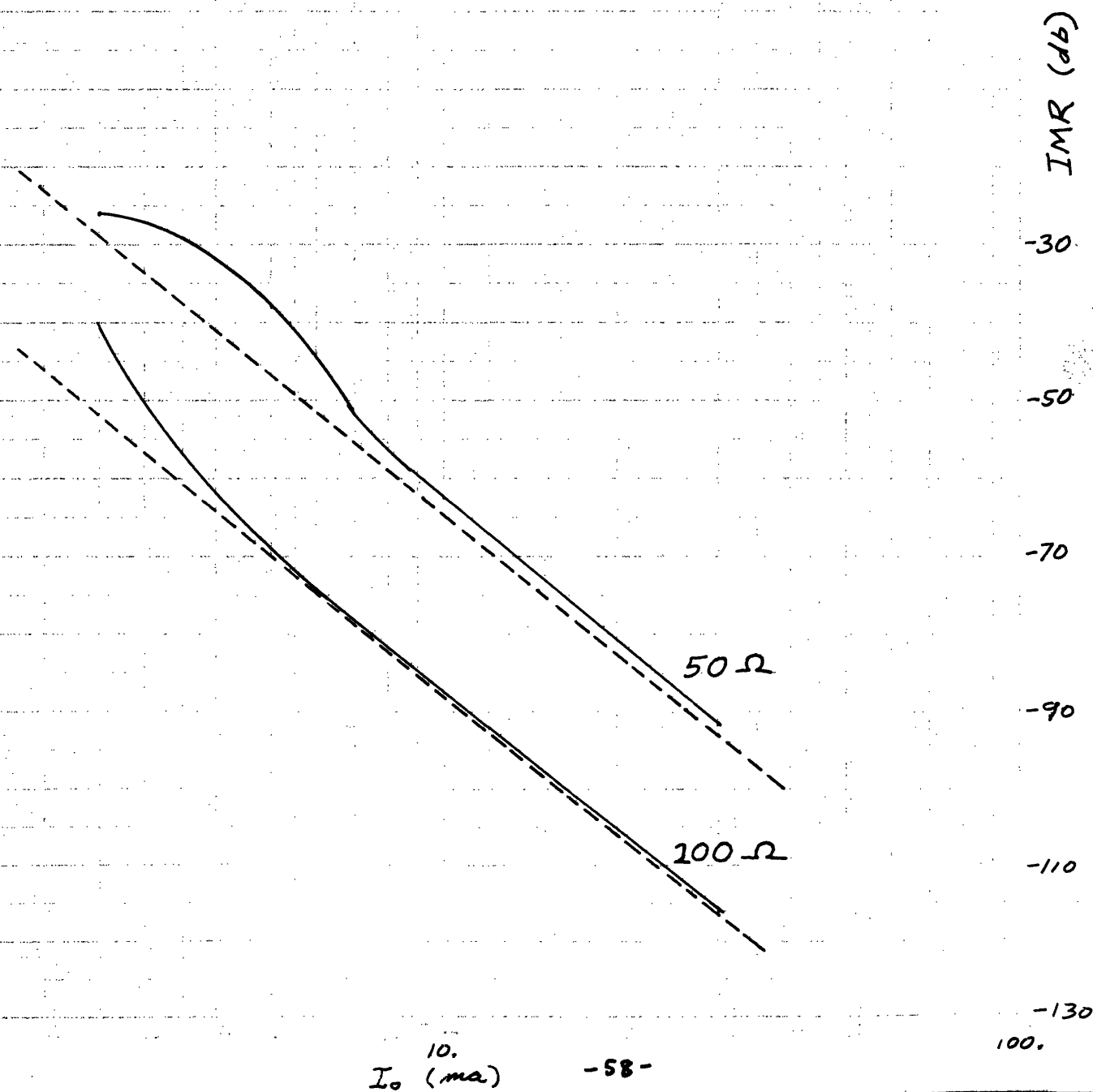
MSQ 5140-2

$f_1 = 30 \text{ MHz}$   
 $f_2 = 32 \text{ MHz}$

FIG. 24 IMR VS. FORWARD  
BIAS CURRENT  
AND SOURCE IMPEDANCE

$P_{in} = -6 \text{ dbm}$

DIODE 2



$I_0$  (mA)

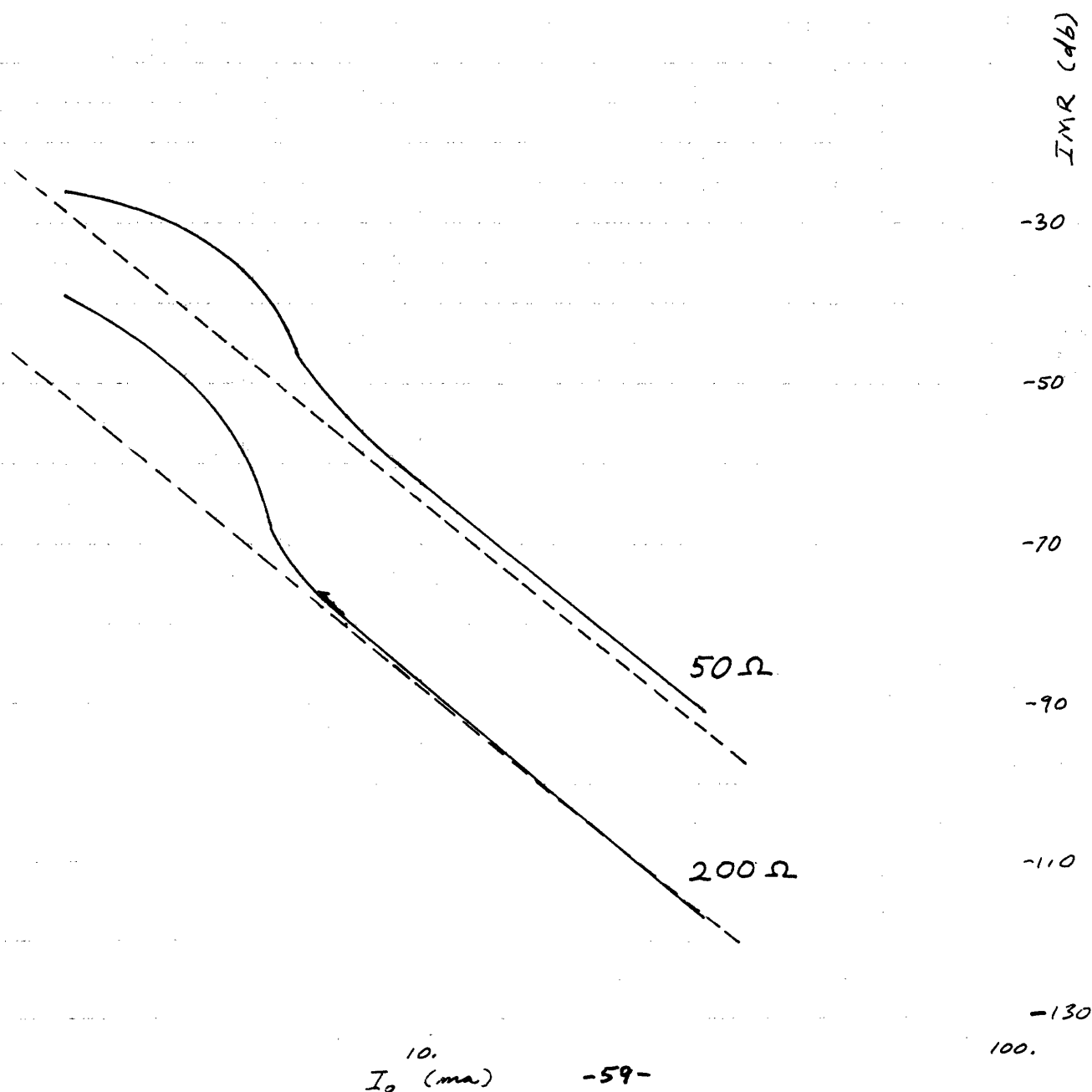
MSQ 5140-3

$f_1 = 30 \text{ MHz}$   
 $f_2 = 32 \text{ MHz}$

FIG. 25 IMR VS. FORWARD  
BIAS CURRENT  
AND SOURCE IMPEDANCE

$P_{in} = -6 \text{ dbm}$

DIODE 3



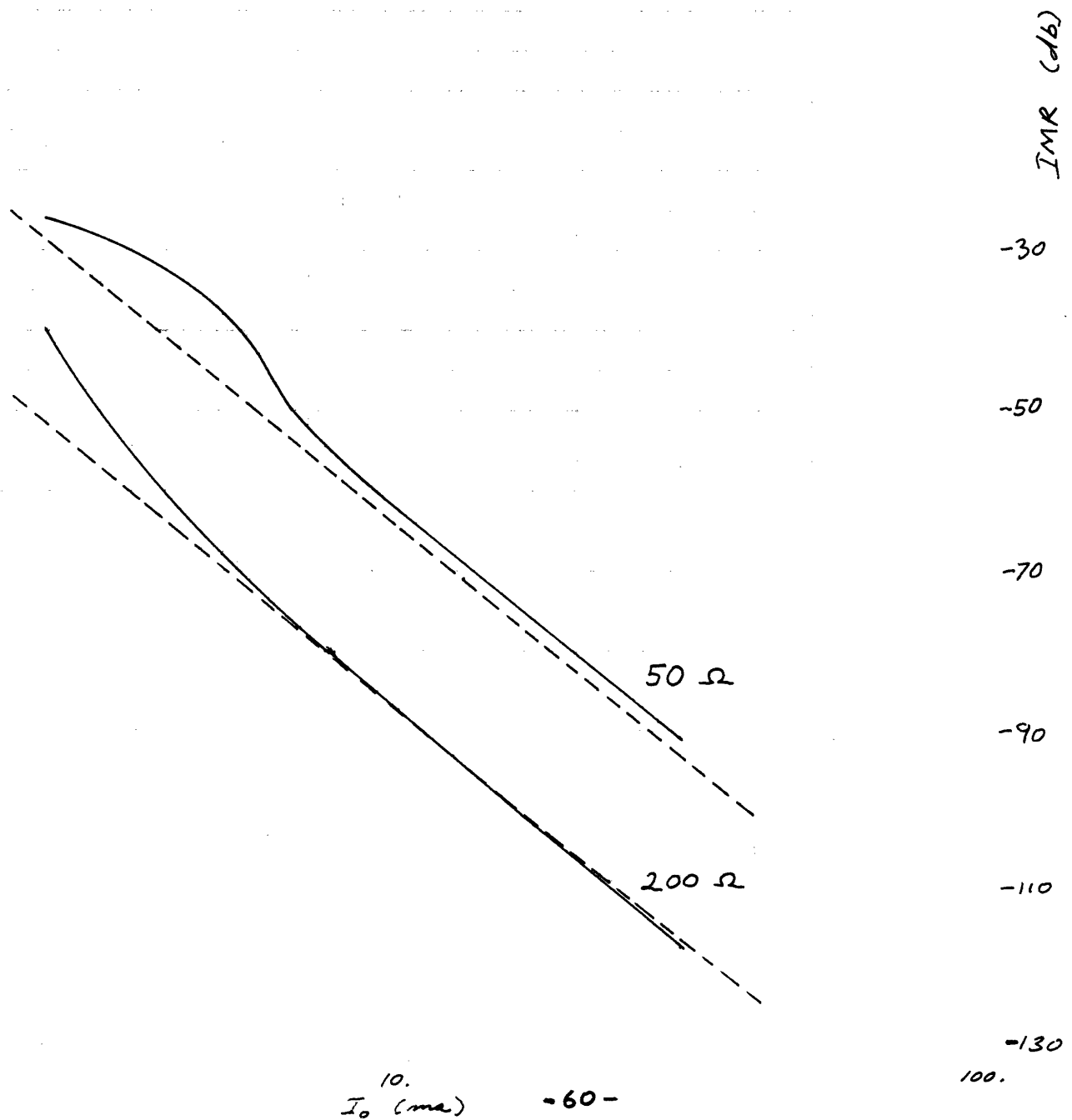
MSQ 5140-4

$f_1 = 30 \text{ MHz}$   
 $f_2 = 32 \text{ MHz}$

FIG. 26 IMR VS. FORWARD  
BIAS CURRENT  
AND SOURCE IMPEDANCE

$P_{in} = -6 \text{ dbm}$

DIODE 4



known. The computer program, in addition to printing out these parameters from the experimental data, also computes standard deviations for the parameters assuming that the experimental data is completely accurate. Using these standard deviations and Eq. 28 an estimated  $\pm 2$  db possible error is found for the reverse biased diode theoretical IM ratios, assuming that there is no error in the diode capacitance measurements.

Fig. 22 shows the IM ratio of one of the MSQ5140 diode vs. forward bias current. Note that from 6 to 30 ma. forward current the IM ratio follows the theoretical prediction to within experimental error. Below 6 ma. transition region IM distortion becomes significant. Between 30 and 40 ma. the IM ratio drops below theoretical, possibly because, as seen in Fig. 11, the series resistance  $R_s$  has increased at this current level. The rapid increase in IM ratio above 40 ma. forward current is not well understood; at this current level considerable diode heating occurs, however, so that considerable changes in several diode parameters may occur. Also shown in Fig. 22 are the IM ratios for one each of the HP2301 and MSQ7330 diodes. Again, the changes in series resistance with forward bias current affect the IM ratio; the continuous decrease of  $R_s$  for the MSQ2330 result in a decreased slope in IM ratio from the theoretical slope of -6. The decrease in  $R_s$  for the HP2301 above 15 ma. results in an increase in IM ratio above 15 ma. for that diode.

The IM ratios for the MSQ5140 diodes in forward bias are plotted in Figs. 23 through 26 at 50 ohm and 200 ohm source impedance levels. These are seen to be close to theoretical in the 6 to 30 ma. region.

The forward bias IM ratio for one of the MSQ5140 diodes is plotted vs. signal input power  $P_{in}$  in Fig. 27. For a 50 ohm source impedance the IM ratio is close to theoretical below a 0 dbm signal level; above that level the transition region IM distortion dominates, until hard clipping is reached in the diode and the IM ratio levels off. For a 200 ohm source impedance, however, the IM ratio is close to theoretical below 0 dbm, but the slope is slightly greater than theoretical. In Fig. 28 the same variables are plotted with the diode in reverse bias. Again, for 50 ohm source impedance, the IM ratio follows the theoretical curve below the transition region. But for a 200 ohm source impedance the slope is slightly greater than theoretical, as in the forward bias case. The voltage step-up in the 200 ohm mixer is apparently large enough to upset the validity of the small signal perturbation assumption, so that a small amount of transition region IM is present, causing this slope discrepancy.

Reverse biased diode IM ratios are plotted vs. bias voltage plus  $\phi$  in Figs. 29 through 32. Transition region IM is dominant below 0.8 volts. Above this voltage the IM ratio is close to theoretical for a 50 ohm source impedance; the difference between theoretical and experimental curves in the 200 ohm case is due to the non-theoretical slope of IMR vs.  $P_{in}$  for 200 ohm source impedance. This is because the IMR at 50 ohms is measured with a 0 dbm two-tone input signal, while that at 200 ohms is measured with a -6 dbm signal.

FIG. 27

IMR VS. SIGNAL INPUT  
POWER AND SOURCE  
IMPEDANCE

FORWARD BIASED  
MSQ 5140-1 DIODE

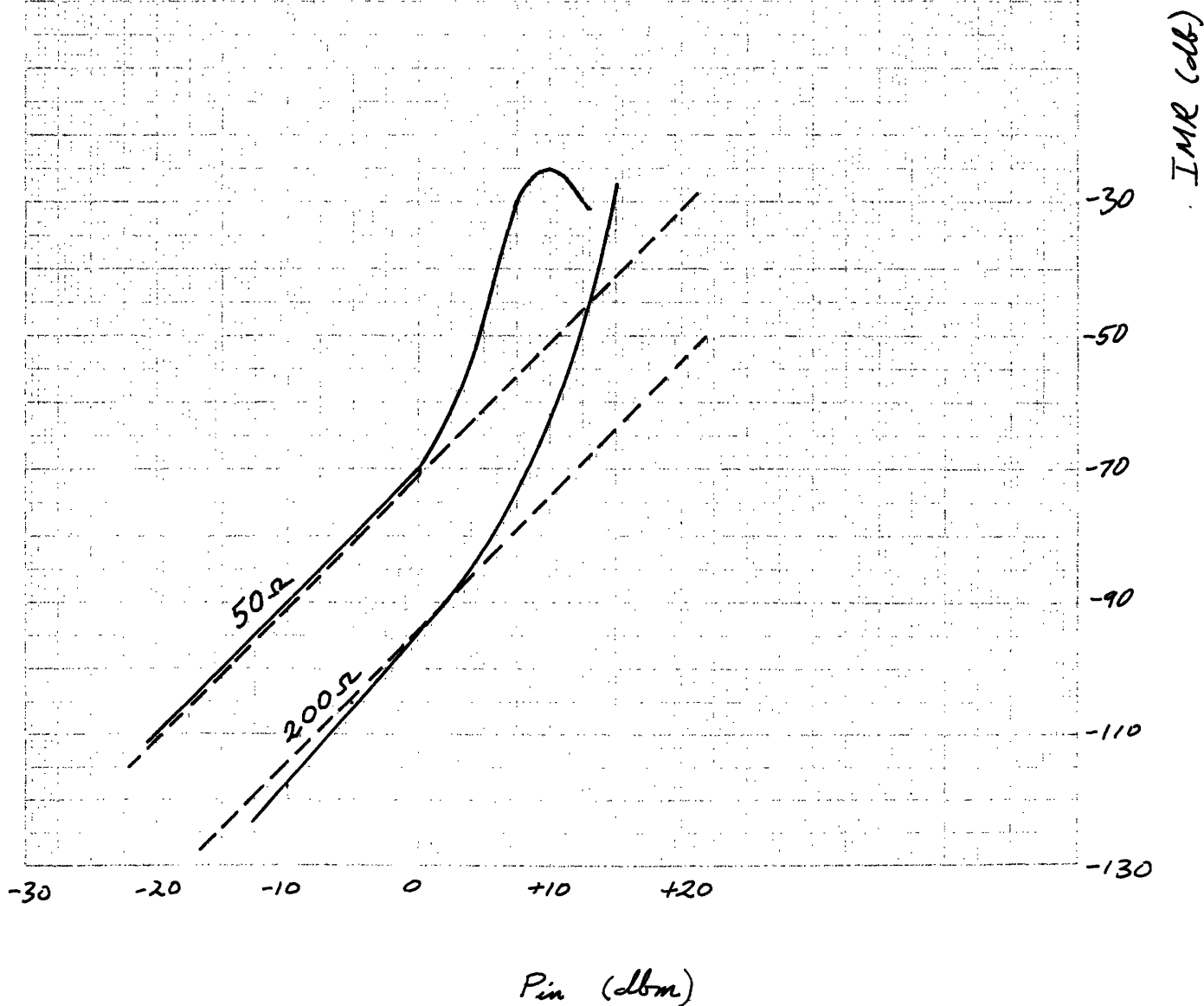
$$f_1 = 30 \text{ MHz}$$

$$f_2 = 32 \text{ MHz}$$

$$I_0 = 20 \text{ ma}$$

$$R_g = 50 \text{ } \Omega$$

$$\pm 200 \text{ } \Omega$$



$P_{in}$  (dbm)

FIG. 28

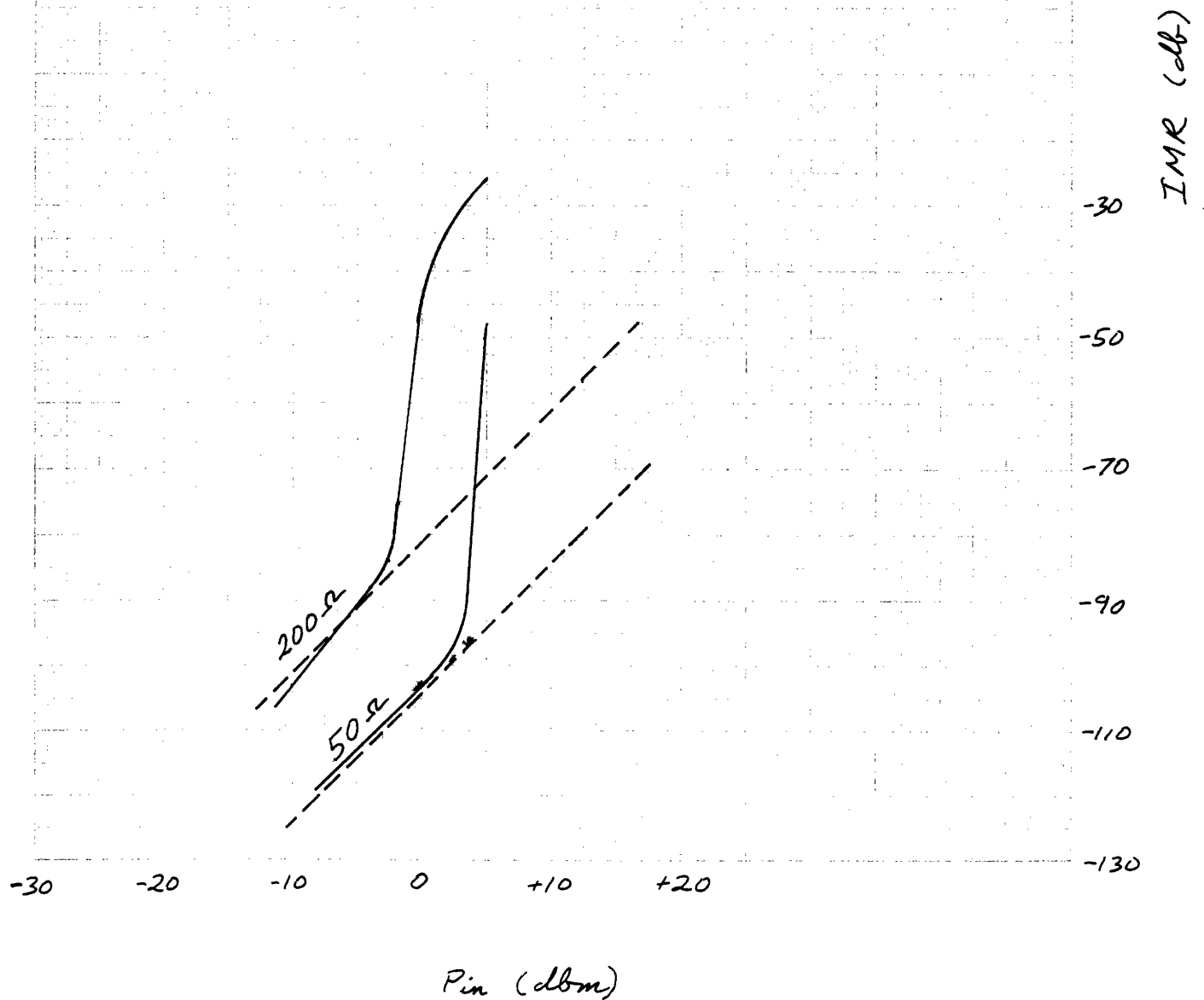
IMR VS. SIGNAL INPUT  
POWER AND SOURCE  
IMPEDANCE

REVERSE BIASED  
MSQ 5140-1 DIODE

$$f_1 = 30 \text{ MHz}$$

$$f_2 = 32 \text{ MHz}$$

$$V_0 = -0.8 \text{ V.}$$



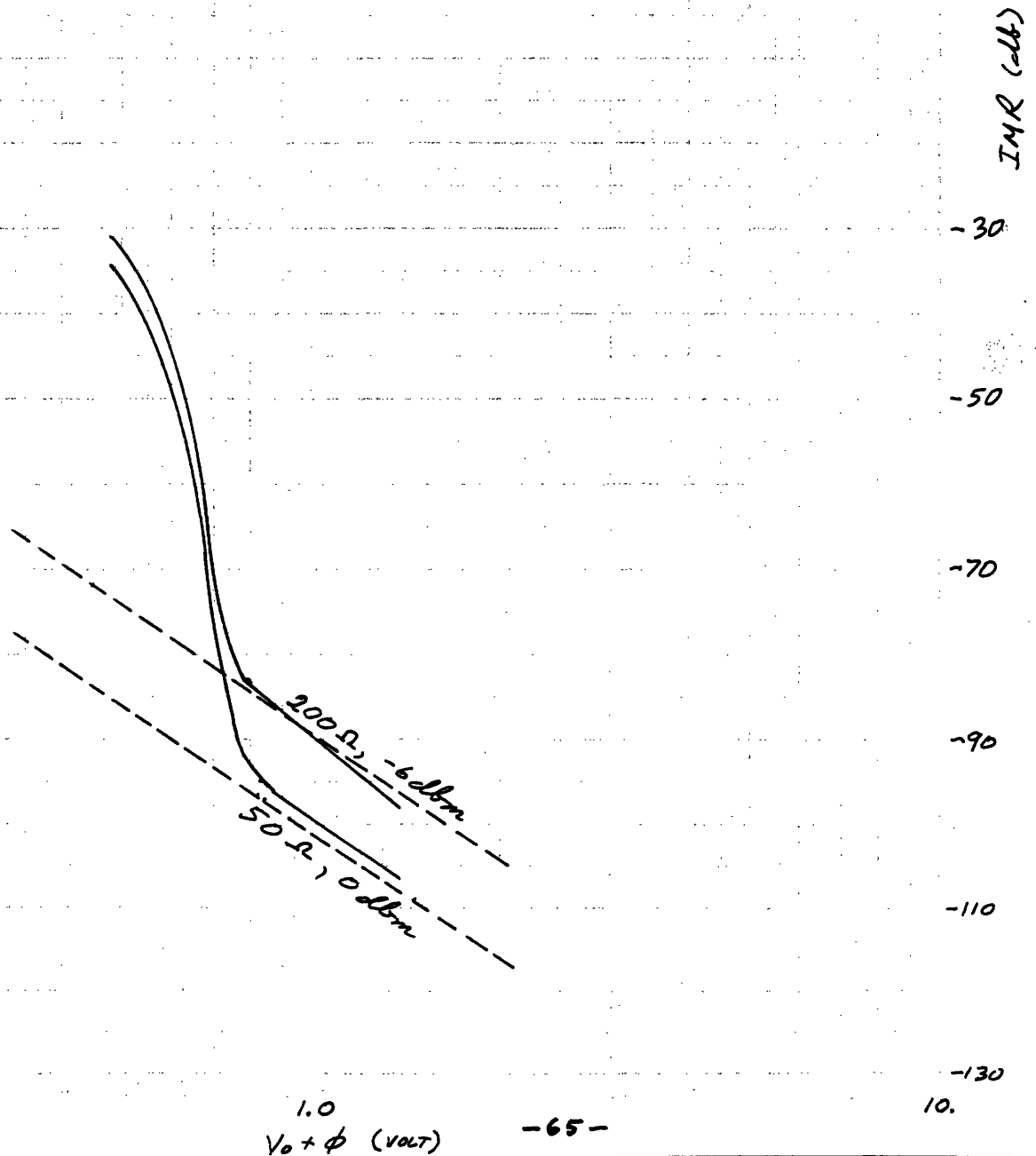


$$f_1 = 30 \text{ MHz}$$

$$f_2 = 32 \text{ MHz}$$

FIG. 29 IMR VS. BIAS VOLTAGE  
AND SOURCE IMPEDANCE

REVERSE BIASED  
MSQ 5140-1 DIODE

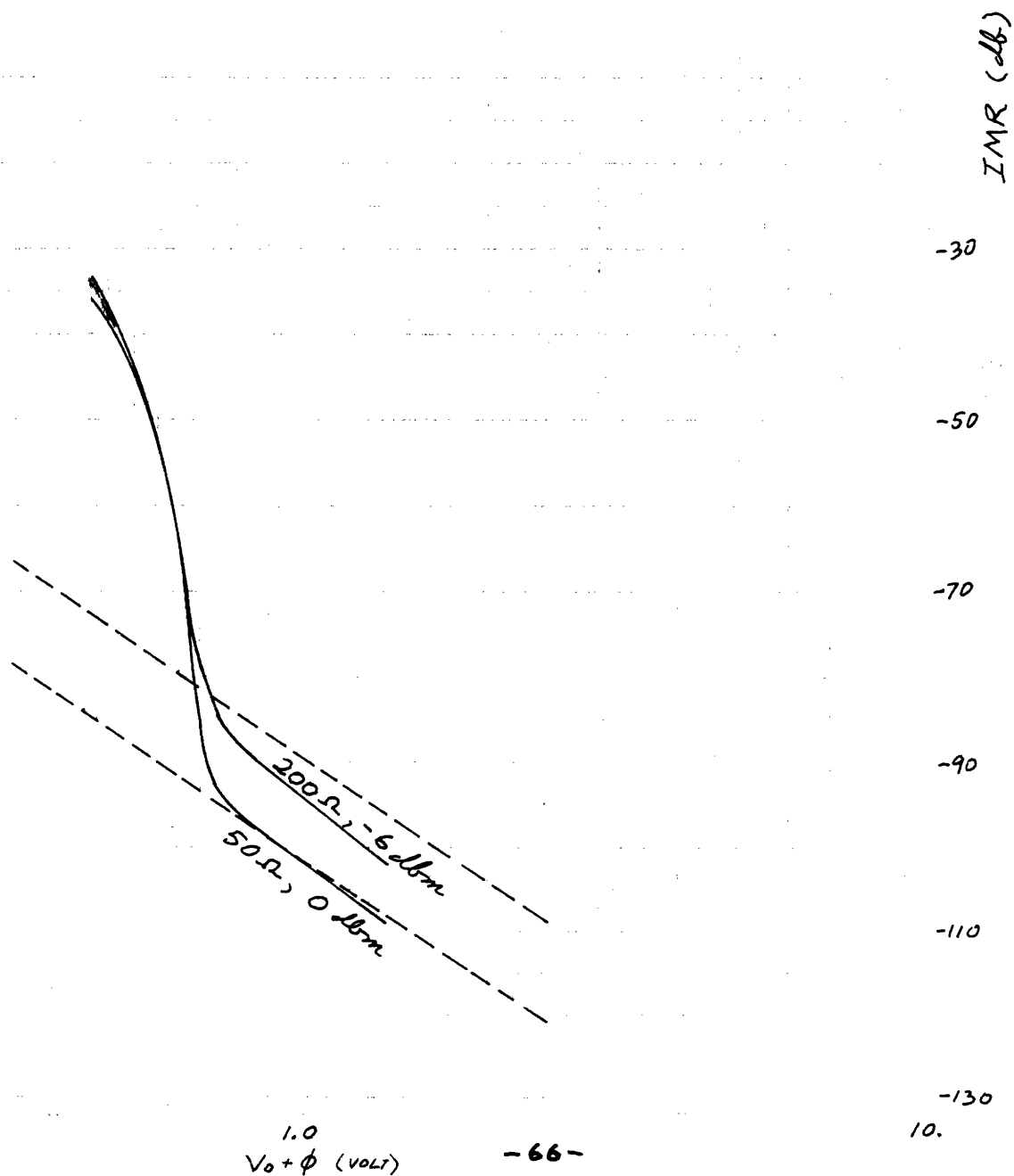


$$f_1 = 30 \text{ MHz}$$

$$f_2 = 32 \text{ MHz}$$

FIG. 30 IMR VS. BIAS VOLTAGE  
AND SOURCE IMPEDANCE

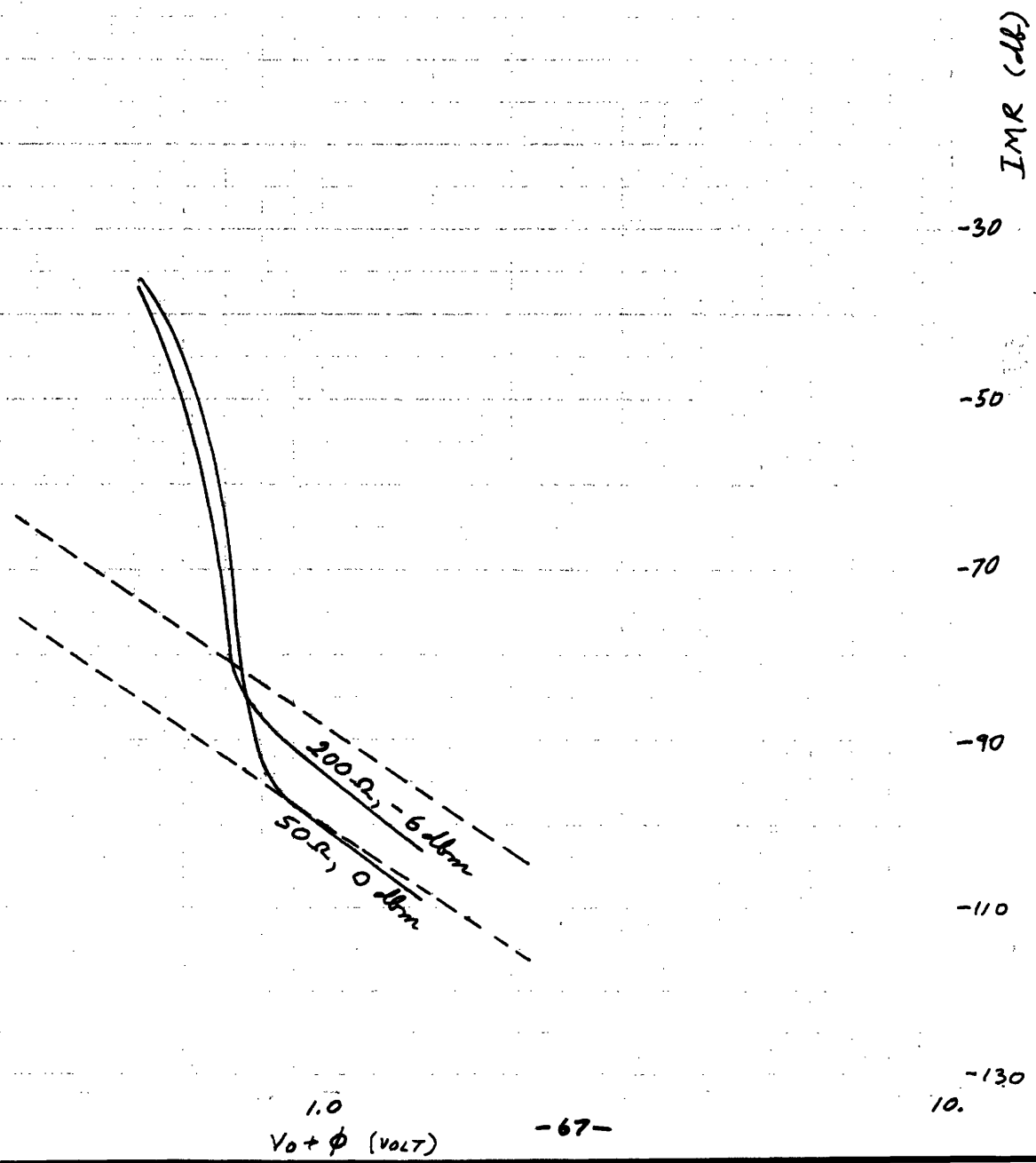
REVERSE BIASED  
MSQ 5140-2 DIODE



$f_1 = 30\text{MHz}$   
 $f_2 = 32\text{MHz}$

FIG. 31 IMR vs. BIAS VOLTAGE  
 AND SOURCE IMPEDANCE

REVERSE BIASED  
 MSQ 5140-3 DIODE

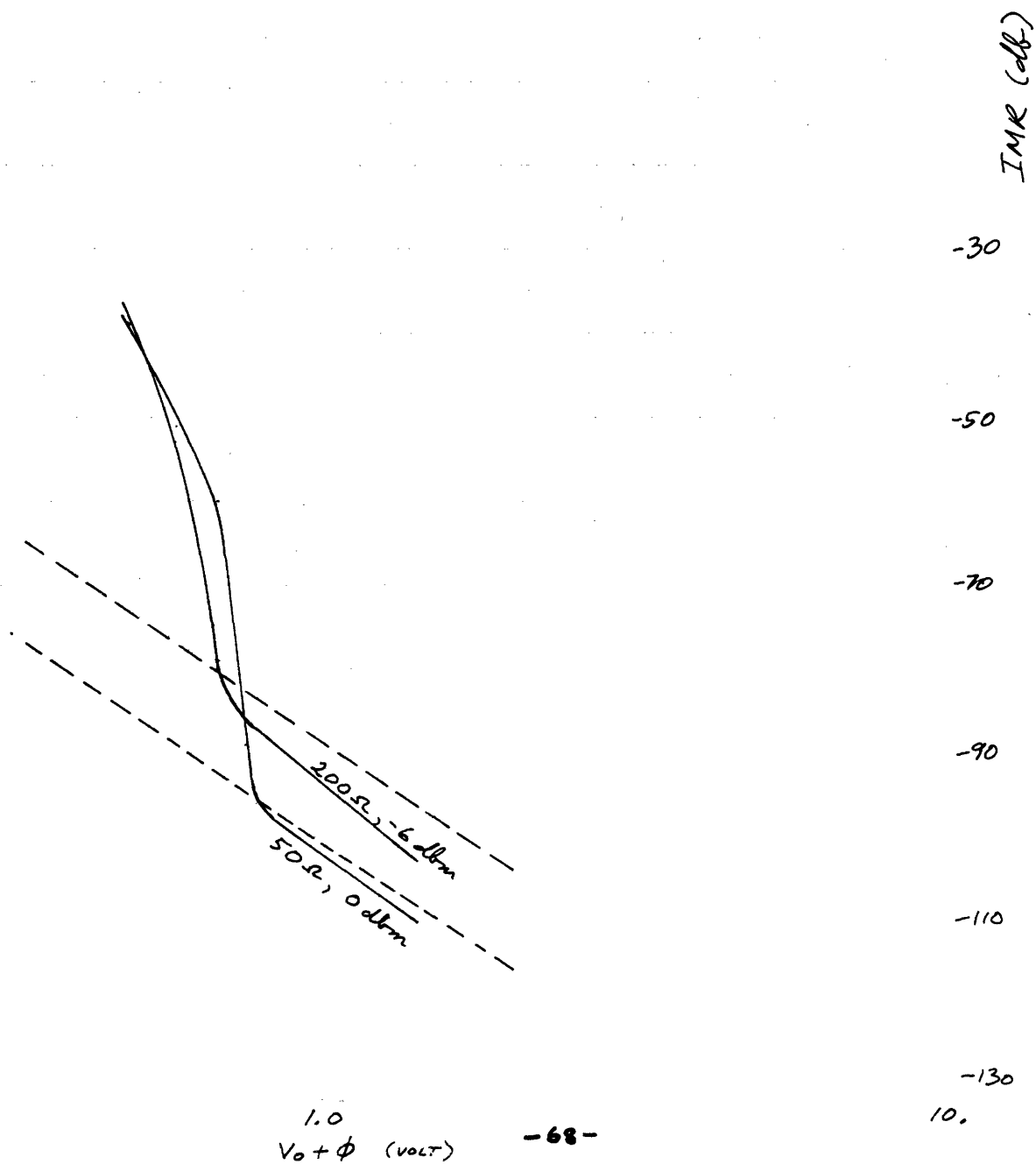


1.0  
 $V_0 + \phi$  (VOLT)

$f_1 = 30 \text{ MHz}$   
 $f_2 = 32 \text{ MHz}$

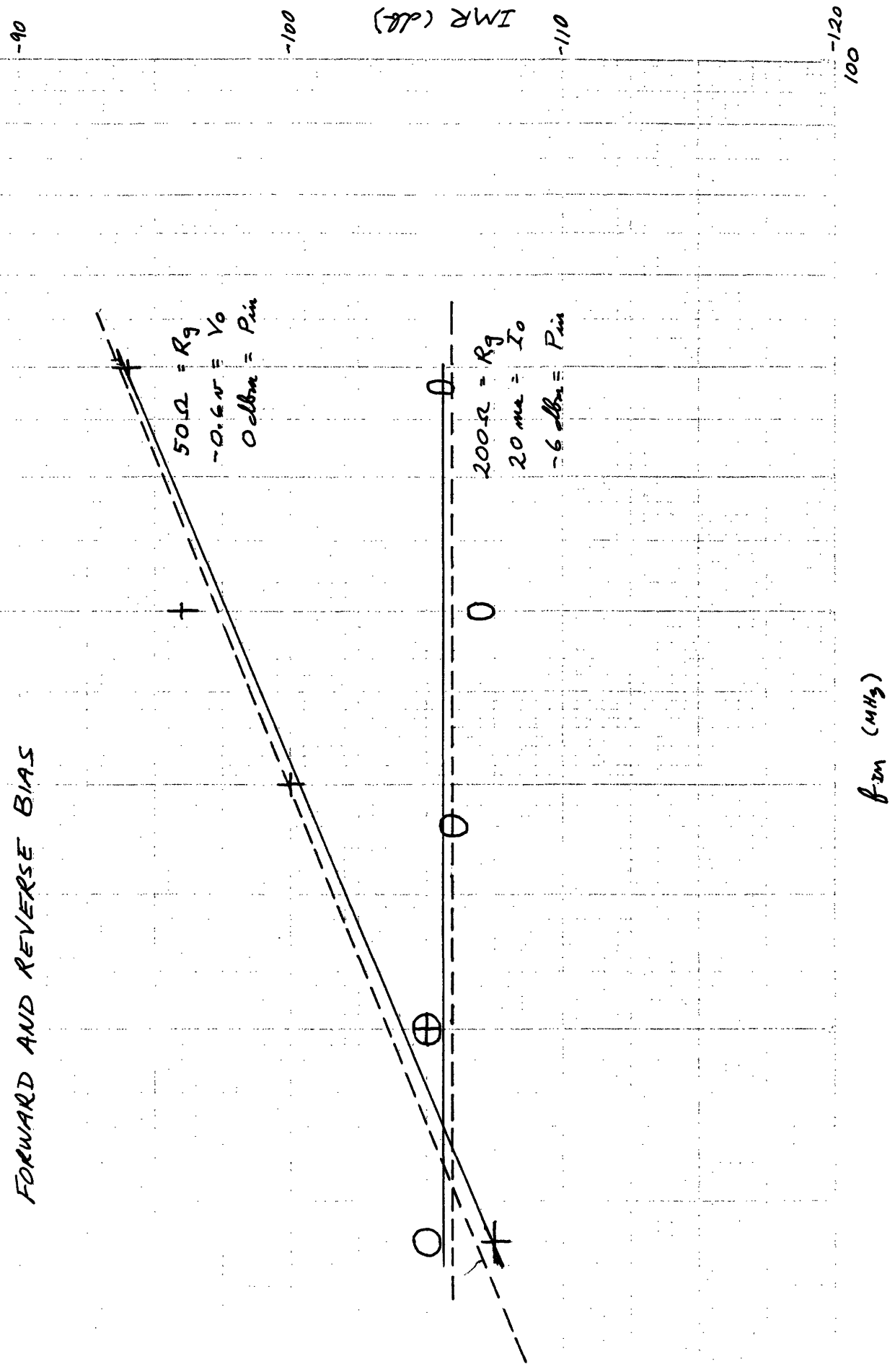
FIG. 32 IMR VS. BIAS VOLTAGE  
 AND SOURCE IMPEDANCE

REVERSE BIASED  
 MSQ 5140-4 DIODE



The frequency dependence of the IM ratio for one of the diodes in forward and reverse bias is shown in Fig. 33. That for the other diodes is similar. As seen, the frequency dependence follows that predicted by theory.

FIG. 33 IMR VS. FREQUENCY FOR  
MSQ 5140-3 DIODE IN  
FORWARD AND REVERSE BIAS



## IM RATIO IN MIXERS

Rather extensive IM measurements were made using the MSQ 5140 diodes in the 50, 100 and 200 ohm mixers. Measurements were made using both sine wave and square wave local oscillators. The amount of LO drive is monitored by measuring the voltage across each diode using a sampling oscilloscope equipped with high impedance differential input probes.

It was discovered that the VSWR of the impedances at the mixer ports is a critical factor in the IM ratio of the mixer. This is caused by reflections which occur at any impedance discontinuities; this reflected power re-enters the mixer to interact with other signals present, and produces additional IM distortion which can either add or subtract from the original distortion, depending on the relative phase angles. Thus, care was taken to insure that reflections at the mixer ports were not affecting the IM ratio.

The results of these measurements are shown graphically in Figs. 34 through 38. In Figs. 34 through 36 the IM ratio for each of the three mixers is plotted as a function of the LO voltage amplitude. The RF signal input power was -10 dbm for the 50 and 100 ohm mixers and -20 dbm for the 200 ohm mixer; the IM frequency was 30 MHz. The IM ratio is plotted using both sine wave and square wave local oscillators. It will be noted that as much as 20 db of improvement in IM ratio results when square wave LO drive is used instead of sine wave drive. Thus it is seen

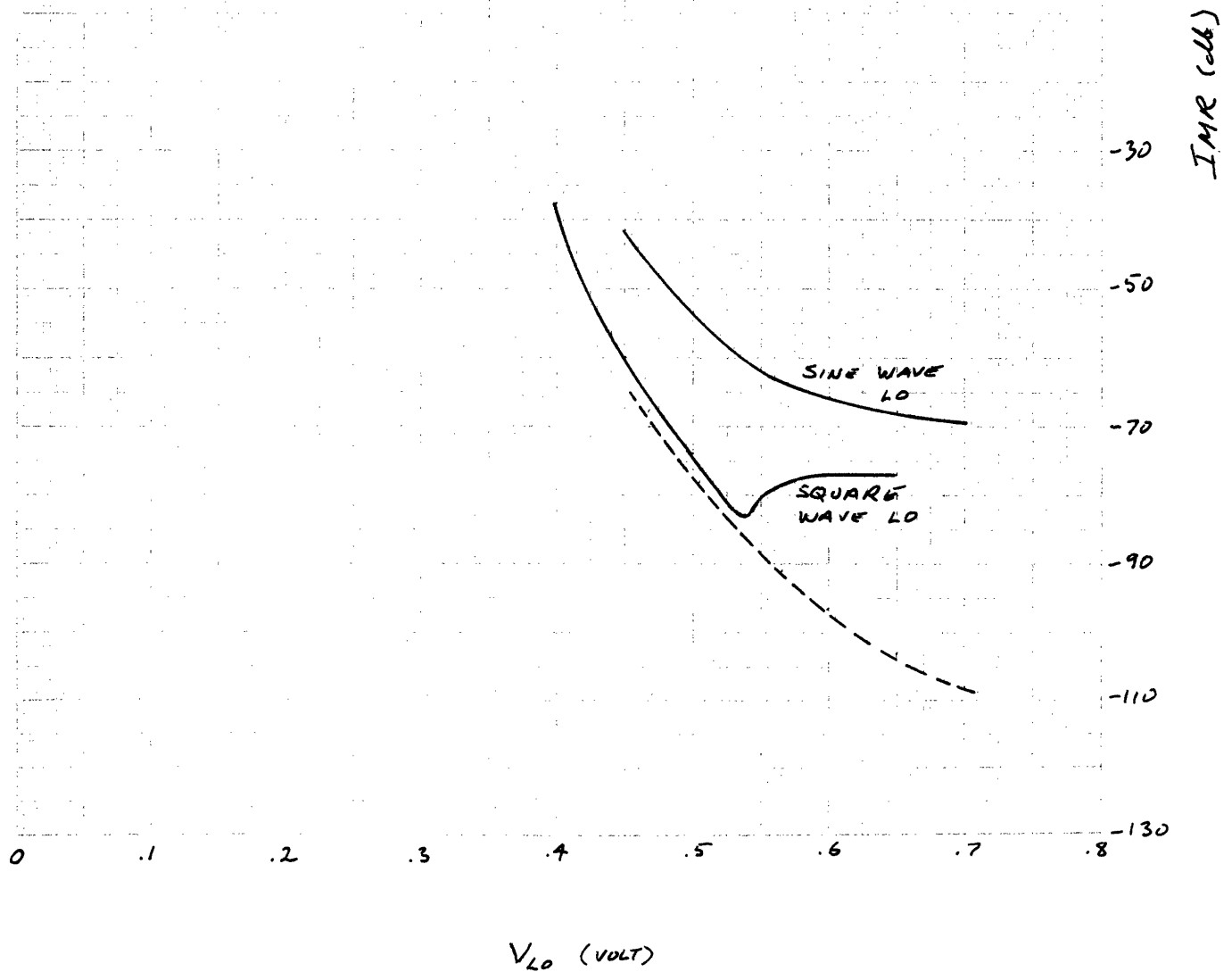
$$R_g = 50 \Omega$$

$$P_{in} = -10 \text{ dbm}$$

FIG. 34 IMR VS. LO VOLTAGE  
ACROSS DIODES

50 $\Omega$  MIXER,

MSQ 5140 DIODES



$V_{LO}$  (VOLT)



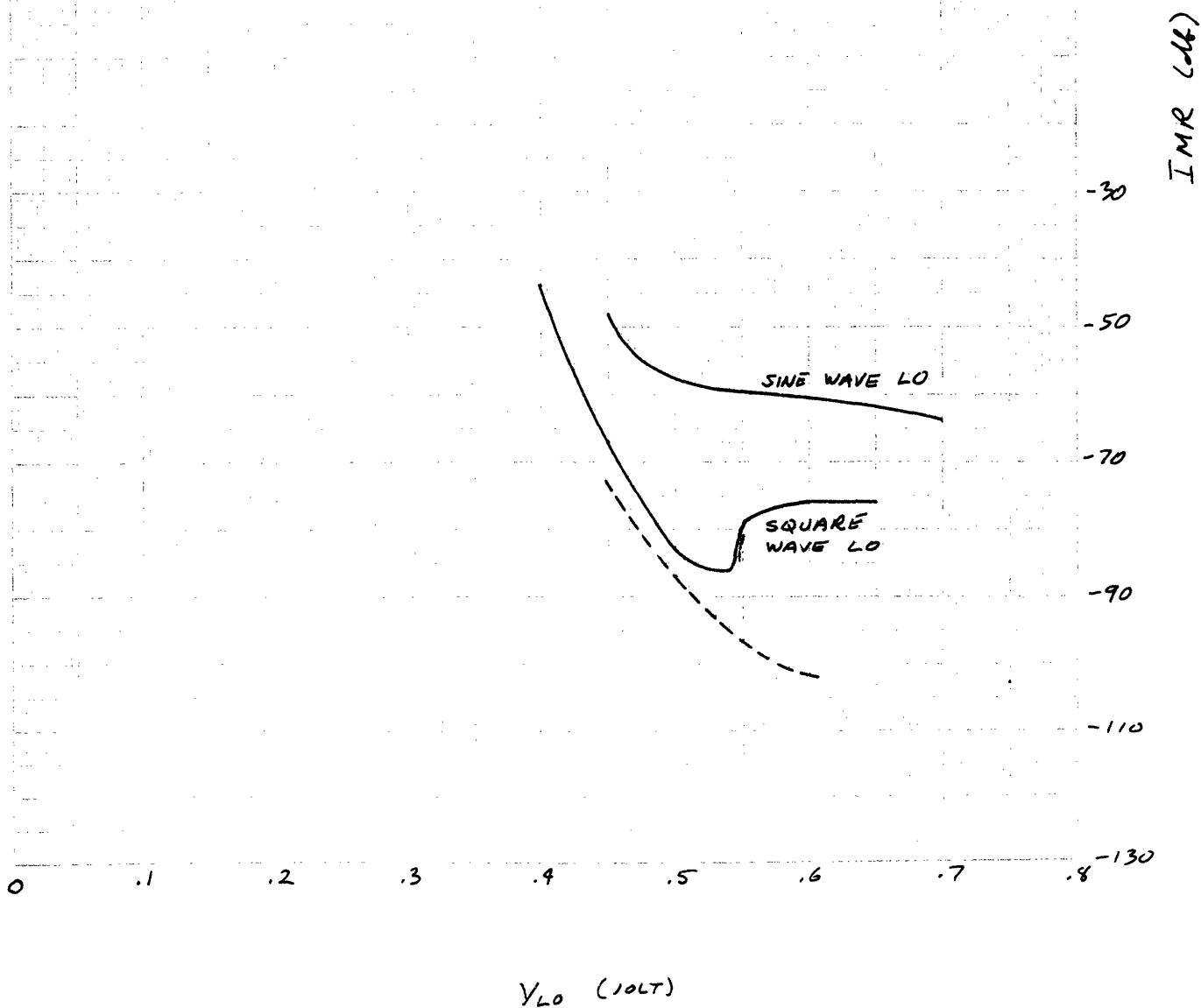
$$R_g = 100 \Omega$$

$$P_{in} = -10 \text{ dbm}$$

FIG. 35 IMR VS. LO VOLTAGE  
ACROSS DIODES

100  $\Omega$  MIXER

MSQ 5140 DIODES



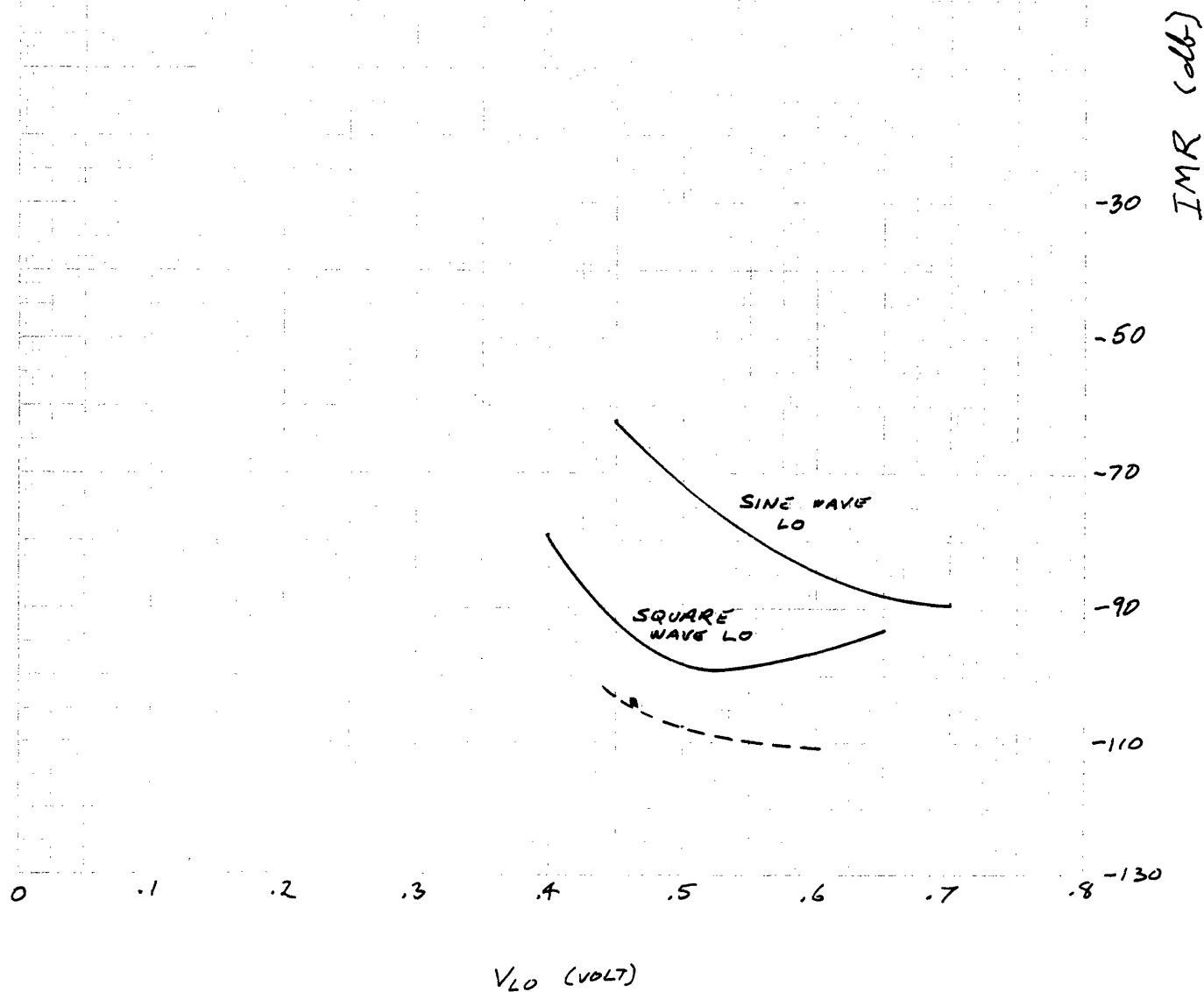
$$R_g = 200 \Omega$$

$$P_{in} = -20 \text{ dbm}$$

FIG. 36 IMR VS. LO VOLTAGE  
ACROSS DIODE

200  $\Omega$  MIXER

MSQ 5140 DIODES



that the transition region is the dominant source of IM distortion in a sine wave driven mixer. There is a 10 db or less discrepancy between theory and measured square wave IM ratio in all three mixers, for LO voltage amplitudes of 0.55 volts or less. The source of this discrepancy is difficult to isolate, but is possibly caused by slight imbalances in the mixer transformers or of the diodes, the presence of transition region IM caused by finite (2 nsec) square wave risetime, or the asymmetry of the square wave generator waveform previously discussed. Adjustment of the symmetry control on the square wave generator changed the IM ratio by less than 2 db, so the last named source is an unlikely one. The small amount of LO and signal frequency feedthrough in the mixers indicates that both the transformers and diodes are well balanced. Thus the most likely source of the discrepancy is the transition region.

Above 0.55 volts LO voltage the IM ratio rises sharply in the 50 and 100 ohm mixers. This rise appears to be the same as that seen in the single diode IM ratios in large forward bias. At large LO drive levels the LO voltage across the diodes becomes rather irregular, with peaks over 30 per cent above the mean voltage level. These peaks are sufficient to drive the forward biased diodes into this region of rapidly rising IM ratio. As Eq. 33 shows, the source of IM in high impedance mixers is primarily the off-biased diode capacitance. This is true for the 200 ohm mixer. Thus the region of rapidly rising IM ratio is greatly suppressed in the 200 ohm mixer.

In Fig. 37 the IM ratio for the MSQ5140 diode mixer is given as a function of source resistance  $R_g$  for two LO drive levels. Note that the difference between experiment and theory increases slightly as the source resistance increases, but that the optimum source resistance remains close to the theoretical values. The 200 ohm mixer data was taken at a -20 dbm signal level, so 20 db was added to the IM ratio to conform with the -10 dbm input levels in the other two mixers.

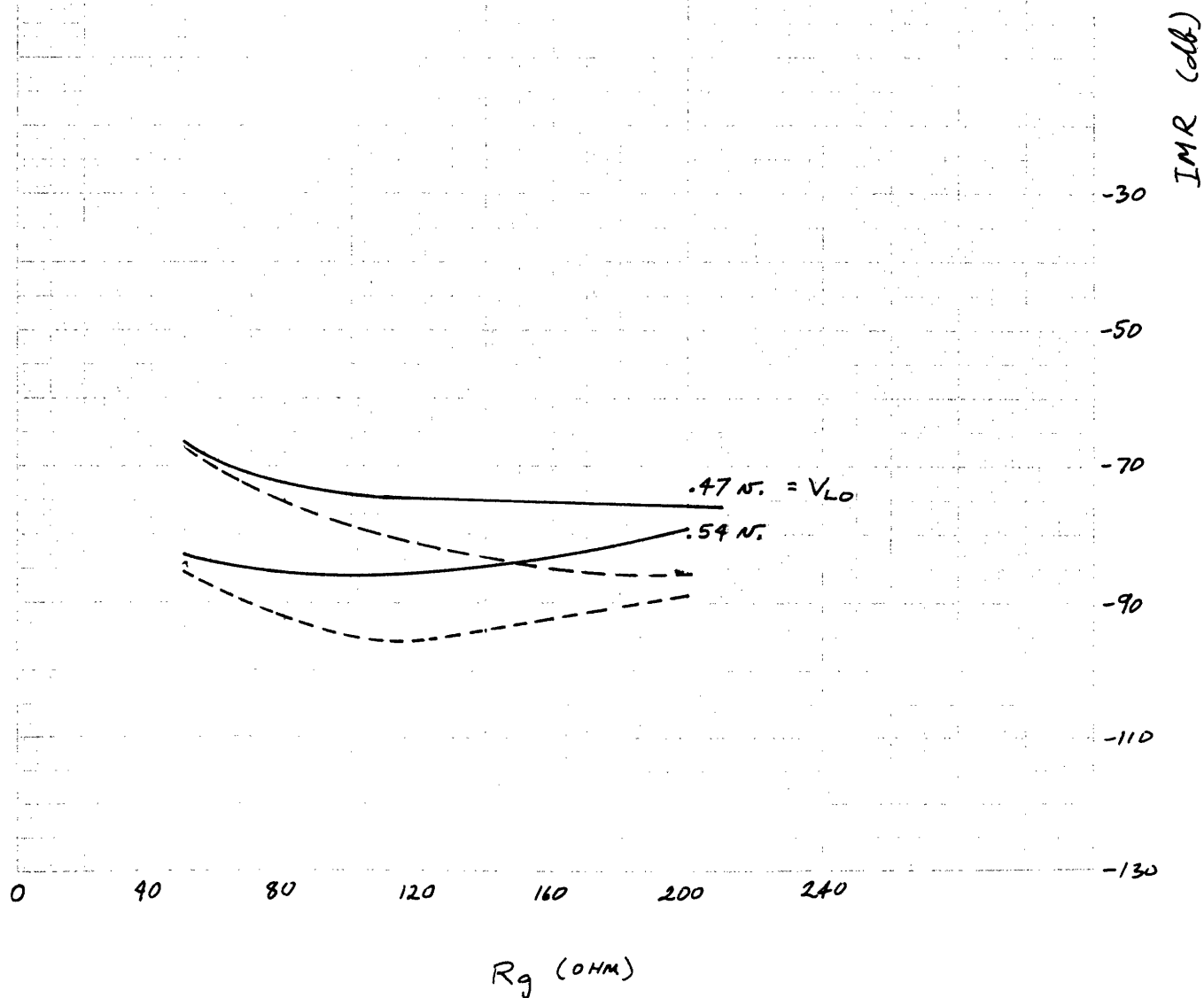
Finally, in Fig. 38 the IM ratio is given for each mixer as a function of the signal power level  $P_{in}$ , for a 0.54 volt LO drive level. The IM ratio is seen to follow the theoretical 2 for 1 slope at low signal levels, but rises faster at higher levels, because the signal level is no longer much smaller than the LO level, as was assumed in the theoretical derivation. The point at which the curve departs from theory goes down in level as the mixer impedance goes up; this is because the transformers that step up the impedance in the mixers also step up the signal voltage.

$$P_{in} = -10 \text{ dbm}$$

$$f_{IM} = 30 \text{ MHz}$$

FIG. 37 IMR VS. SOURCE  
IMPEDANCE AND  
LO VOLTAGE

MSQ 5140 DIODES  
IN MIXERS



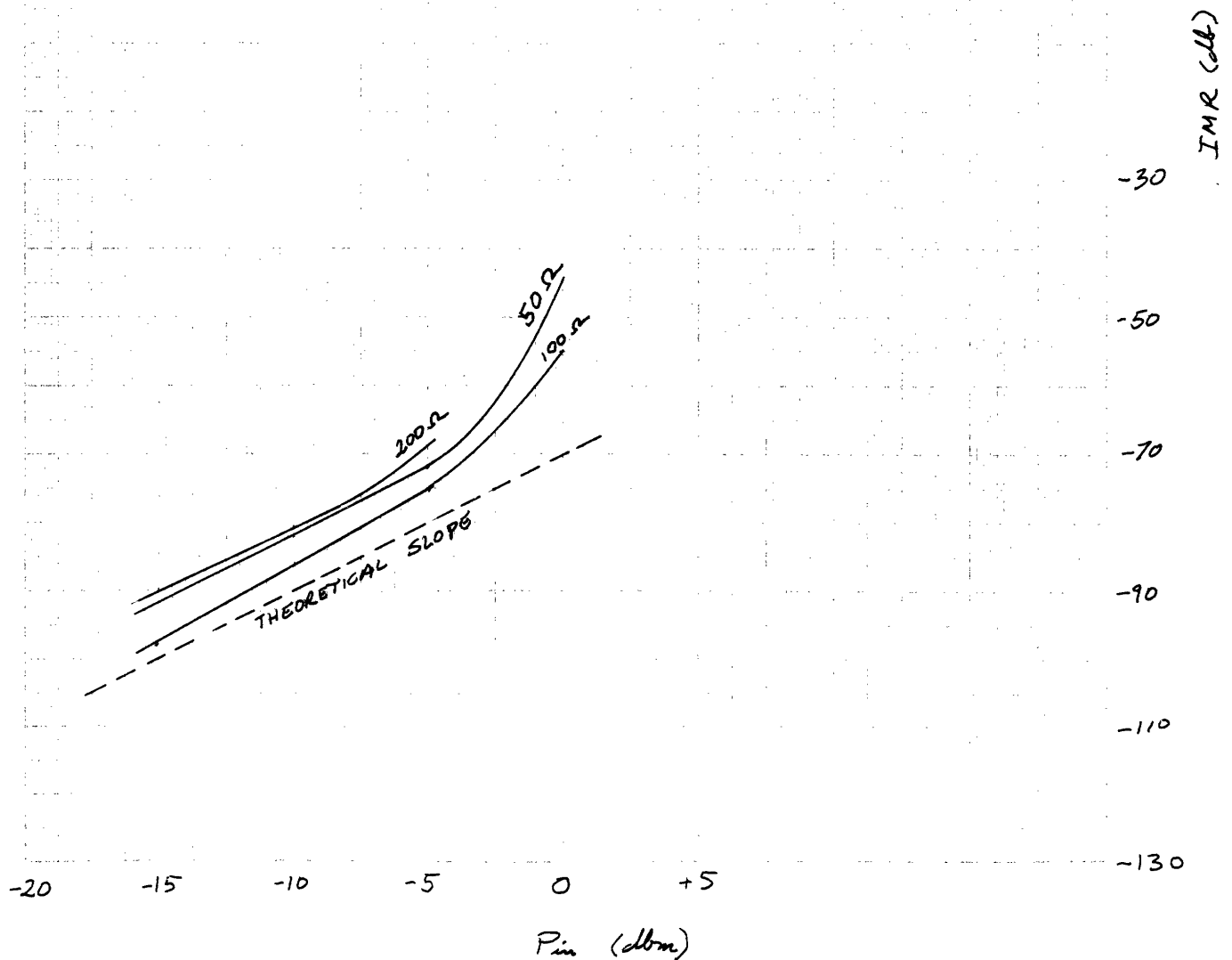
$$f_{IM} = 30 \text{ MHz}$$

$$V_{LO} = 0.54 \text{ V.}$$

FIG. 38

IMR VS. RF SIGNAL  
INPUT POWER AND  
SOURCE IMPEDANCE

MSQ 5140 DIODE MIXERS



## CONCLUSION

As mentioned in the Introduction, the third order IM distortion in mixers is an important factor in determining the mixer's dynamic range. This distortion should be predictable from theoretical considerations if its generation is to be understood and if high dynamic range receivers are to be well designed.

In this thesis a theory for IM distortion in a broad band doubly balanced mixer has been derived using the two-state mixer assumption to identify the sources of IM generation. Diode parameters were measured and used to find the theoretical IM ratio for single diodes in forward and reverse bias, and for the mixer. These were compared with the experimental determinations of IM ratio.

It was found that over a certain range of diode bias voltage and current the IM ratios for single diodes in forward and reverse bias, and for the mixer. These were compared with the experimental determinations of IM ratio.

It was found that over a certain range of diode bias voltage and current the IM ratios for single diodes were quite close to the theoretical predictions. Below this bias range transition region IM distortion became significant; above this range diode heating effects caused a change in the diode's series resistance, which caused the IM ratio to depart from theory since a constant  $R_s$  was assumed. Near the maximum rating of forward current for the diodes a rapid rise in IM ratio was observed. No such departure from theory was observed for the diodes

under large reverse bias, up to the one volt limit to which measurements were made. There was, however, a slight difference in the slope of the IMR vs.  $P_{in}$  curve from the 2 db for 1 db theoretical slope.

The IM ratio for the mixers, however, was as much as 10 db higher than predicted by theory, when square wave LO drive was applied. The most likely explanation for this discrepancy appears to be that the risetime of the square wave local oscillator was not short enough to prevent transition region IM distortion from appearing. At high LO drive levels the mixer IM ratio departed further from theory for low mixer source impedances. This seems to reflect the rapid rise of IM ratio observed in the forward biased diodes at large bias level. The measurements showed a large reduction in IM distortion for square wave as opposed to sine wave LO drive, however, and the optimum source impedance agreed closely with the theory.

Several conclusions may be drawn from these results. First, it may be stated that the third order IM distortion sources in diodes are understood and that, over a range of bias levels, only the sources used in the two-state assumption are significant and are predictable. Second, it was shown that square wave LO drive results in a significant reduction in the IM ratio. Third, it was found that an optimum source impedance exists for a minimum third order IM ratio in the mixer, which depends on the LO drive level in a way that is predictable from theory over a range of LO drive levels. An additional observation which bears restating is that the VSWR's of the three



mixer terminations must be close to unity to prevent multiple reflections from increasing the IM ratio.

Much experimentation is still necessary before IM distortion in diode ring mixers is fully understood. In order to resolve the discrepancy between theory and experiment in mixer IM ratio further work should be done to study the transition region IM. Square wave generators with shorter risetimes may be constructed to see if this discrepancy is indeed due to transition region IM. The frequency dependence of mixer IM should be further studied in an attempt to verify the theoretical predictions already verified in single diodes. The effects on IM ratio of applying negative bias to the mixer diodes should be studied; negative bias should reduce the component of IM distortion due to the reverse diode capacitance. Finally, other types of IM distortion, principally second order, should be investigated, both theoretically and experimentally.

## FOOTNOTES

1. D.H. Steinbrecher, "Mixers", RLE Report, M.I.T., 1968.
2. R.P. Rafuse, "Low Noise and Dynamic Range in Symmetric Mixer Circuits", RLE Report, M.I.T., 1967.
3. R.S. Carruthers, "Copper Oxide Modulators in Carrier Telephone Systems", B.S.T.J. vol. 18 no. 2, pp. 315-337, April, 1939.
4. C.R. Crowell and S.M. Sze, Solid-St. Electron. vol. 9, pg. 1035, 1966.
5. H.C. Torrey and C.A. Whitmer, Crystal Rectifiers, M.I.T. Radiation Laboratory Series, vol. 15. New York: McGraw-Hill, 1948.
6. F.A. Padovani and R. Stratton, Solid-St. Electron. vol. 9, pg. 695, 1966.
7. Handbook of Mathematical Functions, Abramowitz and Stevens, eds., National Bureau of Standards Series, AMS55.
8. A.M. Saleh, PhD Thesis, M.I.T., in progress.
9. J.G. Gardiner, "The Relationship Between Cross-Modulation and Intermodulation Distortions in the Double-Balanced Modulator," P.I.E.E.E., vol. 56 no. 11, pp. 2069-2071, Nov., 1968.
10. A.S. Vander Vorst, "Measurements on Varactors", S.M. Thesis, M.I.T., August, 1965.
11. C.L. Ruthroff, "Some Broad-Band Transformers", P.I.R.E. vol. 47 no. 8, pp. 1337-1342, August, 1959.

#### OTHER REFERENCES

1. W.R. Gretsch, "The Spectrum of Intermodulation Generated in a Semiconductor Diode Junction", P.I.E.E.E. vol. 54 no. 11, pp. 1528-1535, Nov., 1966.
2. D.G. Tucker, Modulators and Frequency Changers, London: Macdonald, 1953.